Revision in the Diprotodontid Marsupial Genus Neohelos: Systematics and Biostratigraphy

Authors: Black, Karen H., Archer, Michael, Hand, Suzanne J., and Godthelp, Henk

Source: Acta Palaeontologica Polonica, 58(4) : 679-706

Published By: Institute of Paleobiology, Polish Academy of Sciences

URL: https://doi.org/10.4202/app.2012.0001

Revision in the diprotodontid marsupial genus *Neohelos*: Systematics and biostratigraphy

KAREN H. BLACK, MICHAEL ARCHER, SUZANNE J. HAND, and HENK GODTHELP

Black, K.H., Archer, M., Hand, S.J., and Godthelp, H. 2013. Revision in the diprotodontid marsupial genus *Neohelos*: Systematics and biostratigraphy. *Acta Palaeontologica Polonica* 58 (4): 679–706.

Neohelos is a geographically and temporally widespread genus of Cenozoic diprotodontid marsupials commonly used to biocorrelate otherwise undated Australian fossil deposits. Here, we revise the genus and describe two new species from the Riversleigh World Heritage Area of northwestern Queensland. *Neohelos solus* sp. nov. is a small, relatively abundant, plesiomorphic form, while the rarer, larger *Neohelos davidridei* sp. nov. is the most derived species of the genus with an upper premolar morphology that is structurally antecedant to members of the Late Miocene genus *Kolopsis*. Additional material of *Neohelos tirarensis* and *Neohelos stirtoni* is described. A chronological morphocline is evidenced by a gradual change in morphology accompanied by an increase in size from *Ne. tirarensis* through *Ne. stirtoni* to *Ne. davidridei*, and is generally consistent with the biostratigraphic distribution of *Neohelos* species throughout Riversleigh's faunal zones A to D. Stage of evolution biocorrelation of *Neohelos* species confirms that some of Riversleigh's Faunal Zone A deposits are Late Oligocene in age and predate the Wipajiri Formation of South Australia. Strong faunal correlations exist between Riversleigh's topographically low to middle Faunal Zone C deposits and the Northern Territory's Middle Miocene Bullock Creek Local Fauna. The presence of the highly derived *N. davidridei* in the Jaw Junction Local Fauna of Riversleigh's Upper Faunal Zone C suggests a later Middle Miocene (post-Bullock Creek) age for this deposit.

Key words: Mammalia, Marsupialia, Vombatomorphia, Diprotodontidae, Zygomaturinae, biocorrelation, systematics, Oligocene, Miocene, Riversleigh, Australia.

Karen H. Black [k.black@unsw.edu.au], Michael Archer [m.archer@unsw.edu.au], Suzanne J. Hand [s.hand@unsw.edu.au], and Henk Godthelp [h.godthelp@unsw.edu.au], School of Biological, Earth & Environmental Sciences, University of New South Wales, Sydney, NSW, 2052 Australia.

Received 4 January 2012, accepted 10 February 2012, available online 17 February 2012.

Introduction

Diprotodontoids (families Diprotodontidae and Palorchestidae) are diverse, extinct, medium- to large-bodied, browsing marsupial herbivores that were widespread and common throughout the Cenozoic of Australia and New Guinea from at least the Late Oligocene. They range from sheep-sized browsers, such as the arboreal *Nimbadon lavarackorum* (Black et al. 2012b), to the three-ton Pleistocene terrestrial *Diprotodon optatum*, the largest marsupial that ever lived, and were key functional components of all of Australia's pre-Holocene terrestrial ecosystems (Black et al. 2012a).

Since 1967, diprotodontoids have been regarded to provide the most reliable tools for biocorrelation of otherwise undated Australian fossil deposits, particularly in the Neogene. The diprotodontoid fauna of the Riversleigh World Heritage Area, northwestern Queensland, is the most diverse currently recorded from any single region in Australia (Black 1997; Black and Hand 2010), with at least 7 genera and 13 species spanning the Late Oligocene to Late Pleistocene. These include the most plesiomorphic (*Propalorchestes*) and derived (*Diprotodon*) diprotodontoids known, and consequently provide an important opportunity to examine key stages in their evolution and use them for continent-wide correlation. Five diprotodontoid species (*Neohelos tirarensis*, *Neohelos stirtoni*, *Nimbadon lavarackorum*, *Ngapakaldia bonythoni*, *Propalorchestes novaculacephalus*) from Riversleigh allow direct biocorrelation with other Tertiary mammal faunas from Queensland, South Australia and the Northern Territory. Of these, species of the zygomaturine genus *Neohelos* Stirton, 1967, have proven most useful, with the chronologic and phyletic succession within the lineage being well documented (Stirton et al. 1967; Murray et al. 2000a, b).

Here, we revise the genus *Neohelos* and describe two new species from Miocene deposits of the Riversleigh World Heritage Area, as well as additional material for *Ne. tirarensis* and *Ne. stirtoni*. We discuss the contribution of the chronological morphocline exhibited by species of *Neohelos* to understanding biostratigraphic relationships within the Riversleigh sequence as well as continent-wide biocorrelation.

http://dx.doi.org/10.4202/app.2012.0001

Institutional abbreviations.—AM F, fossil collection of the Australian Museum, Sydney; AR, temporary paleontological collection of the University of New South Wales, Sydney; CPC, paleontological collection of the Commonwealth of Australia, Canberra; NTM P, paleontological collection of the Northern Territory Museum, Alice Springs; QM F, fossil collection of the Queensland Museum, Brisbane; QM L, fossil locality of the Queensland Museum, Brisbane; SAM P, paleontological collection of the South Australian Museum, Adelaide; UCMP, paleontological collection of the University of California, Berkeley.

Riversleigh Site name abbreviations.—BC2, Black Coffee 2; BO, Burnt Offering; BR, Bone Reef; COA, Cleft Of Ages; CR, Creaser's Ramparts; CS, Camel Sputum; D, Site D; DT, Dirk's Towers; Dun, Dunsinane; FT, Fig Tree; GS, Golden Steph; HH, Henk's Hollow; Inab, Inabeyance; JJ, Jaw Junction; JJS, Jim's Jaw Site; KCB, Keith's Chocky Block; MM, Mike's Menagerie; NG, Neville's Garden; NP, Neville's Pancake; SB, Stick Beak; UBO, Upper Burnt Offering; WH, White Hunter; WW, Wayne's Wok.

Other abbreviations.—FZ, Faunal Zone; I, upper incisor; i, lower incisor; LF, Local Fauna; M, upper molar; m, lower molar; MY BP, million years before present; P, upper premolar; p, lower premolar; WHA, World Heritage Area. Because three key genera discussed throughout this paper begin with "*N*", the following generic abbreviations are used: *Ne.*, *Neohelos*; *Ng.*, *Ngapakaldia*; *Ni.*, *Nimbadon*.

Material and methods

Material described in this work is deposited in the fossil collection of the Queensland Museum, Brisbane, Australia. Much of this material was referred to in Murray et al. (2000b) by temporary (AR) numbers before being accessioned into the Queensland Museum collections. Appendix 1 lists AR numbered specimens noted by Murray et al. (2000b) and their designated QM F numbers. Higher level systematic nomenclature follows Aplin and Archer (1987). Subfamily and generic level nomenclature follows Black and Mackness (1999) who recognize two subfamilies within Diprotodontidae: Diprotodontinae and Zygomaturinae (both originally established by Stirton et al. 1967). Molar homology follows Luckett (1993), where the four permanent molars of the tooth row are numbered M1–4, and the deciduous anteriormost tooth in the cheek tooth row is dP3, which is eventually replaced by P3. Premolar homology follows Flower (1867). Cusp nomenclature follows Archer (1984) and Rich et al. (1978), except that the hypocone of the upper molars is now accepted to be the metaconule following Tedford and Woodburne (1987). Biostratigraphic nomenclature follows Woodburne et al. (1993), Archer et al. (1994, 1997), Creaser (1997) and Travouillon et al. (2006).

Dental measurements were made using CE electronic digital vernier callipers and are standard maximum anteroposterior lengths and buccolingual widths, taken at the base of the crown. In molars, maximum buccolingual anterior widths and posterior widths were taken across the anterior and posterior loph/lophids, respectively. The range of morphological variation in P3 morphology within and between populations is summarized in Table 1 with a comparison of development of P3 cusps, crests and cingula in Riversleigh *Neohelos* samples. Measurements for *Neohelos* spp. (excluding *Ne. stirtoni* from the Bullock Creek LF in the Northern Territory) upper and lower dentitions are given in Appendix 2 (Tables A and B respectively). Measurements of *Ne. stirtoni* dentitions from Bullock Creek are from Murray et al. (2000a: tables 2, 3). Univariate statistics (including coefficients of variation) used to assess whether materials assigned to each species were from single, normally distributed populations were generated using the computer software package PAST (PAleontological STatistics Version 1.51; Hammer et al. 2001). These results are given in Tables 2–4. Bivariate plots of P3–M1 dimensions compare the distribution of *Neohelos* material by site, faunal zone, and species (Fig. 7). P3 and M1 dimensions of Riversleigh *Ne. tirarensis* and *Neohelos* specimens from the Cleft Of Ages LF are compared in Fig. 8.

Systematic paleontology

Superorder Marsupialia Illiger, 1811

Order Diprotodontia Owen, 1866

Family Diprotodontidae Gill, 1872

Subfamily Zygomaturinae Stirton, Woodburne, and Plane, 1967

Genus *Neohelos* Stirton, 1967

Type species: *Neohelos tirarensis* Stirton, 1967; Leaf Locality (UCMP Locality V6213), Kutjamarpu LF, Wipajiri Formation, Lake Ngapakaldi, South Australia; Early Miocene.

Species included.—*Neohelos stirtoni* Murray, Megirian, Plane, and Vickers-Rich, 2000a; *Neohelos solus* sp. nov.; *Neohelos davidridei* sp. nov.

Revised diagnosis.—Species of *Neohelos* are characterized by the following combination of features: four-cusped P3 with a tall, subcentral parametacone, a distinct anterior parastyle, a moderately developed protocone and a small to moderate (though sometimes absent) hypocone; tendency to develop a mesostyle on P3; M1 with well-developed stylar cusp A, stylar cusp E and postmetacrista; M1 with a square occlusal outline (except *Ne. solus*); large interproximal contact between P3 and M1; broad, lanceolate i1 with a ventrobuccal groove and longitudinal lingual crest; and moderate epitympanic fenestra in the postglenoid cavity.

Species of *Neohelos* differ from species of *Silvabestius* in being larger, and in having a distinct parastyle on P3. They differ from species of *Silvabestius* and *Nimbadon*, in having: a broader i1; an increasing posterior molar gradient; a reduced epitympanic fenestra; a moderately inflated postglenoid process; and an obliquely orientated glenoid fossa.

Species of *Neohelos* differ from *Alkwertatherium webbi* in having: a hypocone developed on P3; less oblique molar lophs; a more distinct paracristid on m1; a reduced postparaconal crest on the upper molars; an unconstricted upper diastema; a horizontally aligned basicranial axis; a diastema that does not decline from p3 to i1; and a masseteric foramen developed on the dentary.

Species of *Neohelos* differ from *Plaisiodon centralis* in being smaller and in having: a transverse parametacone crest on P3; a proportionately smaller parastyle on P3; a posteriorly narrow zygomatic arch; and a more open tympanic floor.

Species of *Neohelos* differ from species of *Kolopsis*, *Zygomaturus*, and *Maokopia* in having: an undivided parametacone on P3; a weak digastric fossa and digastric process on the dentary; an open tympanic cavity with a moderately developed epitympanic fenestra; and a shorter, less inflated postglenoid process.

Species of *Neohelos* differ from species of *Hulitherium*, *Maokopia*, and *Zygomaturus* in lacking: divergent I1s; a buccally positioned paracone and metacone on P3; a P3 that is significantly reduced relative to the length of M1; highly inflated frontals and strong frontal crests; a highly flexed basicranial axis; large, elongate, posterior recurved masseteric processes; and a strongly curved, posteriorly deep zygomatic arch.

Species of *Neohelos* differ from *Kolopsoides cultridens* in: having a proportionately shorter P3 relative to M1; having an undivided parametacone on P3; having a weaker parastyle and hypocone on P3; lacking the longitudinal crest linking the apices of the parastyle and paracone on P3; and lacking pointed, recumbent lower incisors.

Geographic and stratigraphic range.—Species of *Neohelos* are recorded from: the Early Miocene Kutjamarpu LF of the Wipajiri Formation, Lake Ngapakaldi, South Australia; the Late Oligocene Kangaroo Well LF of the Ulta Limestone, northwestern Lake Eyre Basin, Northern Territory; the Middle Miocene Bullock Creek LF of the Camfield Beds, Northern Territory; and numerous Late Oligocene to Middle Miocene (FZs A–C) deposits of the Riversleigh WHA, northwestern Queensland. *Neohelos* material is also known from FZs D–E of the Etadunna Formation, central lake Eyre Basin, South Australia, but has yet to be identified to species level.

Neohelos solus sp. nov.

Figs. 1, 2, 9B, Table 1.

2000 *Neohelos* sp. A; Murray et al. 2000a: 31–37, figs. 24–27.

Etymology: From Latin *solus*, alone, the only, which alludes to the fact that this species does not form part of the chronological morphocline, to which all other *Neohelos* species belong.

Holotype: QM F30878, a left partial maxilla with P3, M1–3.

Type locality: Cleft of Ages Site, Riversleigh World Heritage Area fossil deposit; Queensland, Australia.

Type horizon: COA Site is a fissure fill deposit located on the southern section of the Gag Plateau (Creaser 1997). On the basis of vertebrate stage-of-evolution biocorrelation it is tentatively regarded as Middle Miocene (FZ C) in age.

Referred specimens.—From COA Site: QM F40164, Lm1; QM F40158, RM3; QM F40159, Rm1; QM F40160, RM1; QM F40161, RM2; QM F40162, LM1; QM F40163, LM4; QM F56232, RP3; QM F56233, RP3; QM F56234, LP3; QM F56136; Lp3; QM F12432, Lm3; QM F12433, LM4; QM F12434, LM1; QM F20486, Lm1; QM F20488, LM2; QM F20489, Lm3; QM F20490, Rm3; QM F20491, Rm1; QM F20584, RP3; QM F20585, LM2; QM F20709, Rm3; QM F20830, RM2; QM F20831, LM3; QM F20832, Lm3; QM F20838, Lm1; QM F20852, RM1; QM F22765, left partial maxilla with M2–3; QM F22766, Rm2; QM F22767, RM3; QM F22771, RM4; QM F22773, RP3; QM F22774, Rp3; QM F23195, RM1; QM F23197, RM1; QM F23198, Rp3; QM F23199, Rp3; QM F23274, LP3; QM F23407, LM1; QM F23408, RM3; QM F23472, RM1; QM F24270, LM1–3; QM F24298, RP3; QM F24299, RM3; QM F24300, Rp3; QM F24432, Rm2; QM F24433, Rm3; QM F24435, Lm1; QM F24440, Lm4; QM F24667, Rp3; QM F24731, RM1; QM F24741, LM3; QM F29738, Lp3; QM F29739, RM1; QM F29740, RM1; QM F30231, left dentary fragment with m1–2 and partial m3; QM F30305, left maxilla with M1–3; QM F30306, Rm2; QM F30554, Rm1; QM F30556, LM1; QM F30558, RM1; QM F30560, Rm1; QM F30734, RP3; QM F30819, right dentary fragment with m3–4; QM F31356, M1; QM F31357, LM1; QM F31359, Rp3; QM F31364, Rp3; QM F31366, Rm1; QM F36232, Rp3; QM F50481, P3; QM F50487, Rm1; QM F50488, P3; QM F50490, LM2; QM F50492, LM2; QM F50493, LM3. From KCB Site: QM F56138, LP3–M1.

Diagnosis.—*Neohelos solus* differs from other species of *Neohelos* in the following combination of features: small size (except some *Ne. tirarensis*); weak transverse parametacone crest on P3 that does not meet a corresponding crest from the protocone; a tendency to have a more sharply delineated anterobuccal crest on P3; weaker posterobuccal cingulum on P3 that generally lacks a cuspate mesostyle; P3 with a more steeply sloping buccal parametacone surface; proportionately narrower upper molars; shorter, more arcuate protoloph with a deep cleft on its posterior surface on M1–2; a posterolingual metaconule crest that is continuous with the posterior cingulum on M1–2; a discontinuous lingual cingulum on M1; more distinct postparacrista and premetacrista that meet in the interloph valley; more trapezoidal M1–2 in occlusal outline and more convex buccal margins of the paracone and metacone; weaker stylar cusps that are positioned lower on the molar crown; and a higher paralophid and shorter protolophid on m1. *Neohelos solus* differs from *Neohelos davidridei* in having: an undivided parametacone; a P3 with a shorter parastyle that is less separated from the parametacone base; and a p3 with greater emargination between the anterior and posterior tooth moieties.

Description

Holotype.—QM F30878, partial left maxilla with P3, M1–3 (Fig. 1). The dentition is relatively well preserved, except for the absence of enamel on the posterolingual corner of P3 and

http://dx.doi.org/10.4202/app.2012.0001

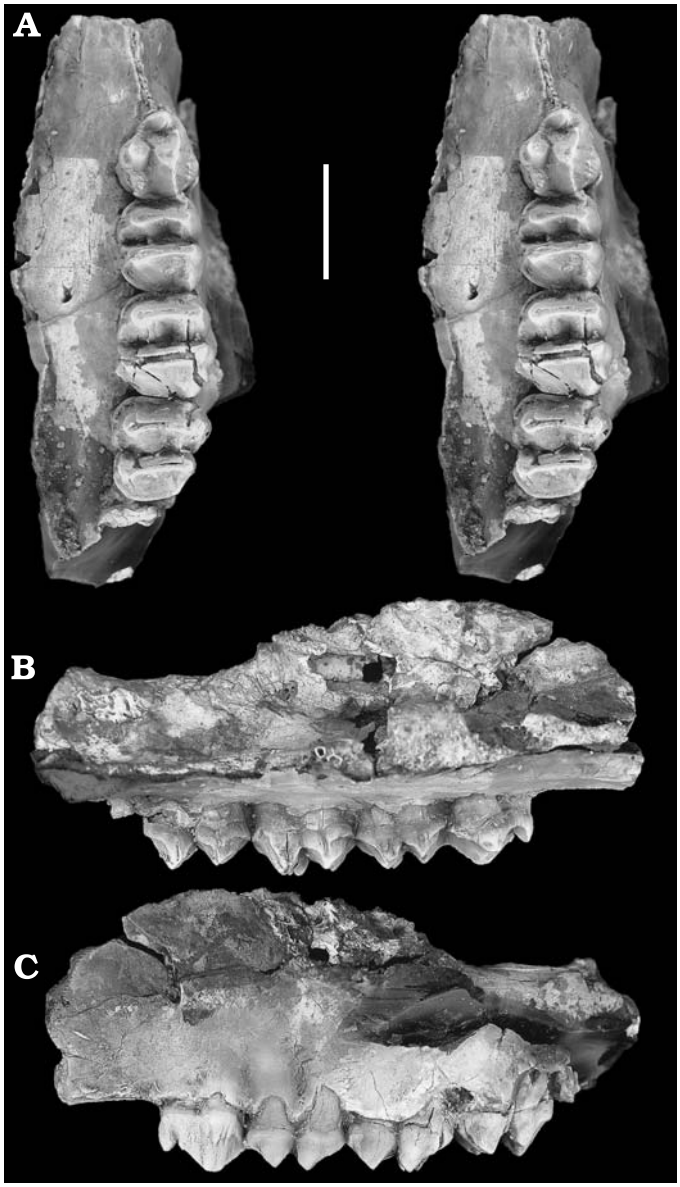

Fig. 1. Diprotodontid marsupial *Neohelos solus* sp. nov. holotype, QMF 30878, partial left maxilla with P3–M3, from the Middle Miocene Cleft Of Ages LF, Riversleigh World Heritage Area, Queensland, Australia. Occlusal stereopair (**A**), lingual (**B**), and buccal (**C**) views. Scale bar 20 mm.

some slight fracturing of enamel on the posterobuccal and anterobuccal margins of M2 and M3, respectively. The cheek tooth row is relatively straight along its lingual margin, but slightly convex along its buccal margin. A slight, posteriorly increasing molar gradient is evident. A large, ovate (9.5 × 4.5 mm) infraorbital foramen is positioned 14.4 mm above the anterior root of P3. A round (4.9 mm diameter) infraorbital canal opens 34.5 mm posterior to the infraorbital foramen on a rounded sub-orbital shelf that is scarred by nutrient foramina.

P3 (Fig. 1): The premolar is a small, sub-ovate tooth with four main cusps: a tall, central parametacone; moderate lingual protocone; small, erect, anterior parastyle; and a weak posterolingual hypocone. The apices of all these cusps show moderate wear. A distinct anterobuccal crest from the parametacone apex terminates in the transverse valley separating the bases of the parastyle and parametacone. A stronger posterobuccal parametacone crest extends to the posterior tooth border where it meets the parastyle of M1, and is continuous with a weak posterolingual cingulum. A buccal cingulum is absent, however, a swelling at the base of the crown, opposite the parametacone apex, may represent a weak mesostyle. The enamel in this area is strongly ridged. The lingual base of the protocone is bulbous. The buccal base of the protocone is separated from the parametacone by a moderately deep cleft. There is no evidence of a transverse crest linking the apices of the protocone and parametacone, but there may have been a weak anterolingual parametacone crest. The anterolingual cingulum is thick but low, dominated by a series of vertical ridges in the enamel, and continuous with a vertical crest which ascends the lingual face of the parastyle.

M1 (Fig. 1): M1 is elongate and trapezoidal in occlusal outline, with a narrow anterior protoloph and a wider posterior metaloph. Both lophs are moderately worn, particularly on their anterior faces. The protoloph is crescentic (compared with the relatively linear metaloph), creating a deep cleft on its posterior face at the midline of the tooth. The transverse median valley is moderately deep, convoluted, and open buccally. A weak lingual cingulum is formed by the junction of a posterolingual protocone crest and anterolingual metaconule crest. The enamel on the lingual faces of the protocone and metaconule is heavily ridged. A well-developed posterior crest descends the lingual face of the metaconule and becomes continuous with the posterior cingulum. A weaker anterior cingulum is also present. The parastyle and metastyle are distinctly cuspate, but situated low on the crown. The metastyle is connected to the metaloph by a weak, elongate postmetacrista.

M2 (Fig. 1): M2 is similar to M1, except that it is larger overall and proportionately wider, with a wider protoloph and metaloph. The parastyle and metastyle are reduced, as are the preparacrista and postmetacrista. The buccal tooth margin is more bulging and convex and the transverse median valley is more deeply convoluted. The posterior face of the metaloph is steeper and narrower.

M3 (Fig. 1): Similar to M2, except that the metaloph is much narrower than the protoloph and more obliquely orientated, resulting in a more trapezoidal occlusal outline. The transverse median valley is wider and open lingually and the parastyle and metastyle are further reduced.

Referred material.—Dentary: Description based on QM F30231 (Fig. 2) and QM F30819. The partial left dentary QM F30231 preserves the area of the horizontal ramus below m1 to the posterior border of m3, but is missing the inferior border and much of the surface bone on its lingual face. The dentary is moderately deep and the lateral surface of the horizontal ramus is broadly rounded below m3. The medial surface of the horizontal ramus is relatively flat. QM F30819, a right partial dentary, preserves the area posterior to m3 and anterior to the (secondary) masseteric foramen. The dentary is moderately deep (42.3 mm taken between m3 roots) and

Table 1. Comparison of the size and development of structures on the upper third premolar of species of *Neohelos*. Abbreviations: L, large; M, medium; m, moderately developed; opp., opposite; pa-me, parametacone; S, small; st, strong; w, weak; XL, extra large; XS, extra small; "+", present; "–", absent; "?", indeterminate owing to wear or breakage; *estimated.

	Specimen	Faunal Zone	Site	Size	L	W	Parastyle		Hypo-cone	Meso-style	Postero-buccal cingulum	Buccal swelling	Parametacone transverse crest	
					mm		size	structure					Develop-ment	Meets the protocone
Neohelos solus	QM F56232	?C	COA	S	14	12.4	S	erect	?	+	w	opp. pa-me	w	+
	QM F56233	?C	COA	S-M	15.2	12.8	M	erect	M	–	–	posterior	w	–
	QM F56234	?C	COA	S	14.3	12.4	S	erect	–	–	w	opp. pa-me	w	+
	QM F20584	?C	COA	S	14.8	13.4	M	?	M	+	st	posterior	w	+
	QM F 22773	?C	COA	S	14.1	12.6	S	?	M	–	–	posterior	w	–
	QM F23274	?C	COA	S	14.6	12.6	M	erect	M	–	w	opp. pa-me	w	–
	QM F30734	?C	COA	S-M	15.5	13.8	XS	hooked	XS	–	w	opp. pa-me	st	–
	QM F30878	?C	COA	S	14.4	12.9	S	erect	S	–	–	opp. pa-me	w	–
	QM F50481	?C	COA	S	14.2	12	M	hooked	S	–	w	opp. pa-me	w	–
	QM F50488	?C	COA	S	14.6	13.5	M	?	?	–	w	opp. pa-me	w	–
	QM F56138	?C	KCB	S-M	15.1	15.1	S	erect	–	–	w	opp. pa-me	w	–
Neohelos tirarensis	Holotype	N/A	Leaf	M	?	14.8	?	?	S	+	m	opp. pa-me	w	+
	AMF87625	N/A	Leaf	M	15.8	13.9	S	hooked	S	+	m	opp. pa-me	w	+
	QM F40130	A	SB	S	?	12.3	S	?	S	+	m	posterior	w	+
	QM F40131	A	SB	S	14.5	13	S	erect	S	–	st	posterior	w	–
	QM F40132	A	BR	S	14.3	13.4	S	hooked	–	–	w	opp. pa-me	w	–
	QML935	?A	Dun	M	16.3	14.3	L	hooked	M	+	st	opp. pa-me	st	+
	QM F56236	B	CR	M	16.6	13.6	M	erect	S	–	w	opp. pa-me	st	+
	QM F40137	B	CS	M-L	17	14.1	M	?	M	–	w	opp. pa-me	st	+
	QM F40136	B	CS	M	?	?	M	erect	?	?	?	?	?	?
	QM F40133	B	CS	M	16.6	14.7	M	erect	S	+	st	opp. pa-me	w	+
	QM F56237	B	DT	S	14.8	13.4	M	erect	M	+	m	opp. pa-me	st	+
	QMF13088	B	In	M	16.4	14.3	M	hooked	M	+	st	opp. pa-me	st	+
	QM F40150	B	MM	M	16.8	13.6	M	erect	S	–	–	opp. pa-me	w	+
	QM F40151	B	MM	M	15.6	14.8	S-M	hooked	M	+	–	opp. pa-me	w	+
	QMF56135	B	WW	M	16.3	15	M	erect	M	–	–	opp. pa-me	w	+
	QMF23157	?B	FT	S	14.3	13.4	S-M	?	S	–	m	posterior	st	+
	QM F40145	C	JJS	M	16.8*	12.9	M	hooked	S	–	w	opp. pa-me	w	+
	QMF36321	?C	BC2	M	16.9	15.5	L	erect	S	+	st	opp. pa-me	w	+
	QM F56137	?C	KCB	M-L	17.5	14.8	L	?	M	–	m	opp. pa-me	w	+
	QM F56238	?C	KCB	M	16.1	14.2	M	erect	M	+	m	opp. pa-me	w	–
Neohelos stirtoni	QM F40165	C	Gag	M-L	17.1	14.4	L	hooked	S	–	–	opp. pa-me	w	+
	QM F40168	C	Gag	L	17.5	16.1	S-M	erect	XS	+	m	opp. pa-me	w	–
	QM F40167	C	HH	L	19.2*	?	M	erect	S	?	?	?	w	+
Neohelos davidridei	QM F40175	C	JJ	XL	20.7	16.6	L	erect	M	+	w	opp. pa-me	–	–
	QM F40178	C	JJ	XL	20.8	16.8*	L	hooked	M	+	st	opp. pa-me	w	–

broadly rounded (23.6 mm) with a broad lateral shelf beside the molar row. Medially, the dentary drops away steeply below m3–4. The ascending ramus originates 15 mm lateral to the interloph valley of m4 and rises at an angle of 70° relative to the occlusal molar plane. The post-alveolar shelf is 14.5 mm long, yet the post-alveolar process is weak. The pterygoid fossa extends anteriorly below the level of the post-alveolar process. In cross section, the internal mandibular canal is large and ovate (9.1 mm high × 5.6 mm wide). A small masseteric foramen (1.8 mm diameter) is situated 17.0 mm posterior to the anterior border of the masseteric fossa. A smaller (1.5 mm diameter) secondary masseteric foramen lies 4.6 mm posterior to the first. Both foramina are confluent with the mandibular canal internally.

p3: Description based on QM F31359, QM F36232 (Fig. 2) and QM F31364 (right p3s) and QM F56136 (left p3). The p3 is a two-rooted, sub-ovate tooth, dominated by a central protoconid which is connected to a shorter posterior cuspid by a concave crest. In all specimens, the anterior border of the protoconid descends steeply to the base of the crown. In QM

http://dx.doi.org/10.4202/app.2012.0001

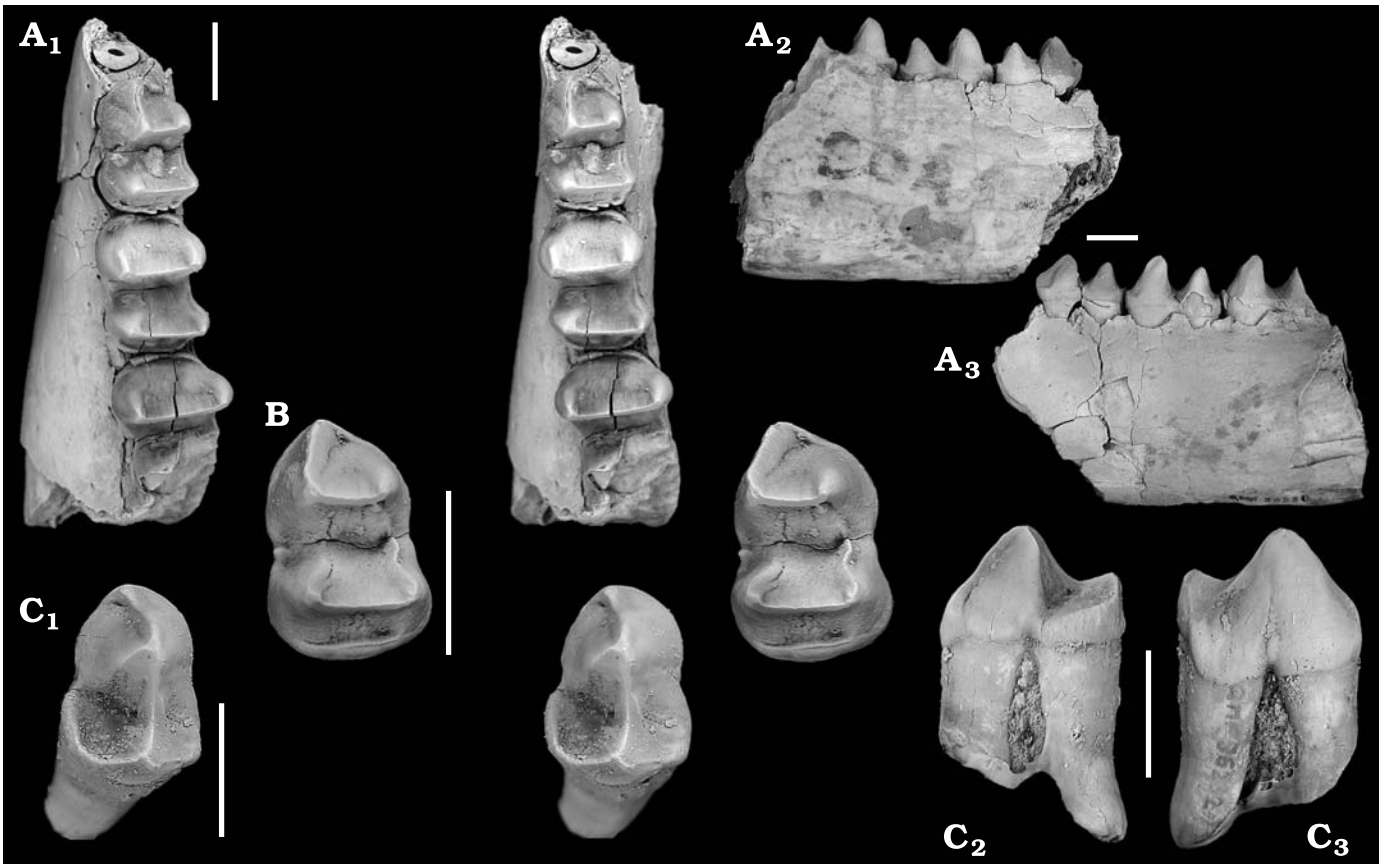

Fig. 2. Diprotodontid marsupial *Neohelos solus* sp. nov. from the Middle Miocene Cleft Of Ages LF, Riversleigh World Heritage Area, Queensland, Australia. **A**. QMF30231, partial left dentary with m1–2, partial m3; occlusal stereopair (A_1), buccal (A_2), and lingual (A_3) views. **B**. QMF31357, Lm1; occlusal stereopair. **C**. QMF36232, Rp3; occlusal stereopair (C_1), lingual (C_2), and buccal (C_3) views. Scale bars 10 mm.

F31359 and QM F31364, it is convex in lateral profile, whereas in QM F36232 and QM F56136 it is straighter and terminates in a slight swelling at the base of the crown. A well-developed lingual fossa is present in all, and is defined anteriorly by a lingual cristid from the protoconid apex, posteriorly and lingually by a well-developed cingulum, and buccally by the posterior protoconid crest. In QM F31364, the lingual fossa is deeper and better delineated owing to a steeper posterior protoconid crest and lingual protoconid cristid.

m1: QM F31357 (left m1, Fig. 2), QM F31366, and QM F50487 (right m1s). The m1 is a two-rooted, sub-rectangular tooth with a narrow, elongate trigonid (consisting of a transverse protolophid and an anteriorly directed paralophid) and a broader talonid (consisting of a transverse hypolophid). QM F31366 and QM F31357 are unworn specimens and both possess high paralophid crests. In QM F31366 the paralophid is continuous with the anterolingual cingulum, however in QM F31357, an anterolingual cingulum is absent. In all specimens, the preentocristid is well-developed and terminates in the interloph valley, and a slightly cuspate buccal cingulum is present, albeit to varying degrees. QM F50487 is a slightly broader tooth overall.

m2–3: Description based on QM F30231 (Fig. 2), a left dentary fragment with m1–2 and partial m3, and QM F30819, a right dentary fragment with m3–4. The m2 and m3 are two-rooted, sub-rectangular teeth with broad anterior protolophids and narrower posterior hypolophids. Low, broad anterior and posterior cingula are present. The interloph valley is broadly V-shaped (in lateral view) and open, owing to the absence of buccal and lingual cingula. QM F50408, a left m3, is similar to QM F30819, but larger overall.

m4: Based on QM F30819. Similar to m3, yet slightly narrower with a more reduced hypolophid.

Remarks.—QM F30878 (Fig. 1), here designated as the holotype of *Neohelos solus*, was nominated by Murray et al. (2000b) as a reference specimen for *Neohelos* sp. A. Extended descriptions of the following referred material (representing i1, p3, m1–4, P3, M1–4), can be found in Murray et al. (2000b): QM F20488; QM F20584; QM F20585; QM F20828; QM F20852; QM F23197; QM F23274; QM F24230; QM F30305; QM F30557; QM F30734; QM F69257. Additional referred material recovered since submission of MAGNT Report 6 is described in Appendix 3 in so far as it differs from the holotype, and includes QM F56232-4, QM F31356, QM F50481, QM F50486, QM F50488, QM F50490 and QM F50492-3, all from the COA LF, and QM F56138, from the KCB LF.

Geographic and stratigraphic range.—Middle Miocene; COA and KCB sites (FZ C), southern section of the Gag Plateau, Riversleigh World Heritage Area, northwestern Queensland, Australia.

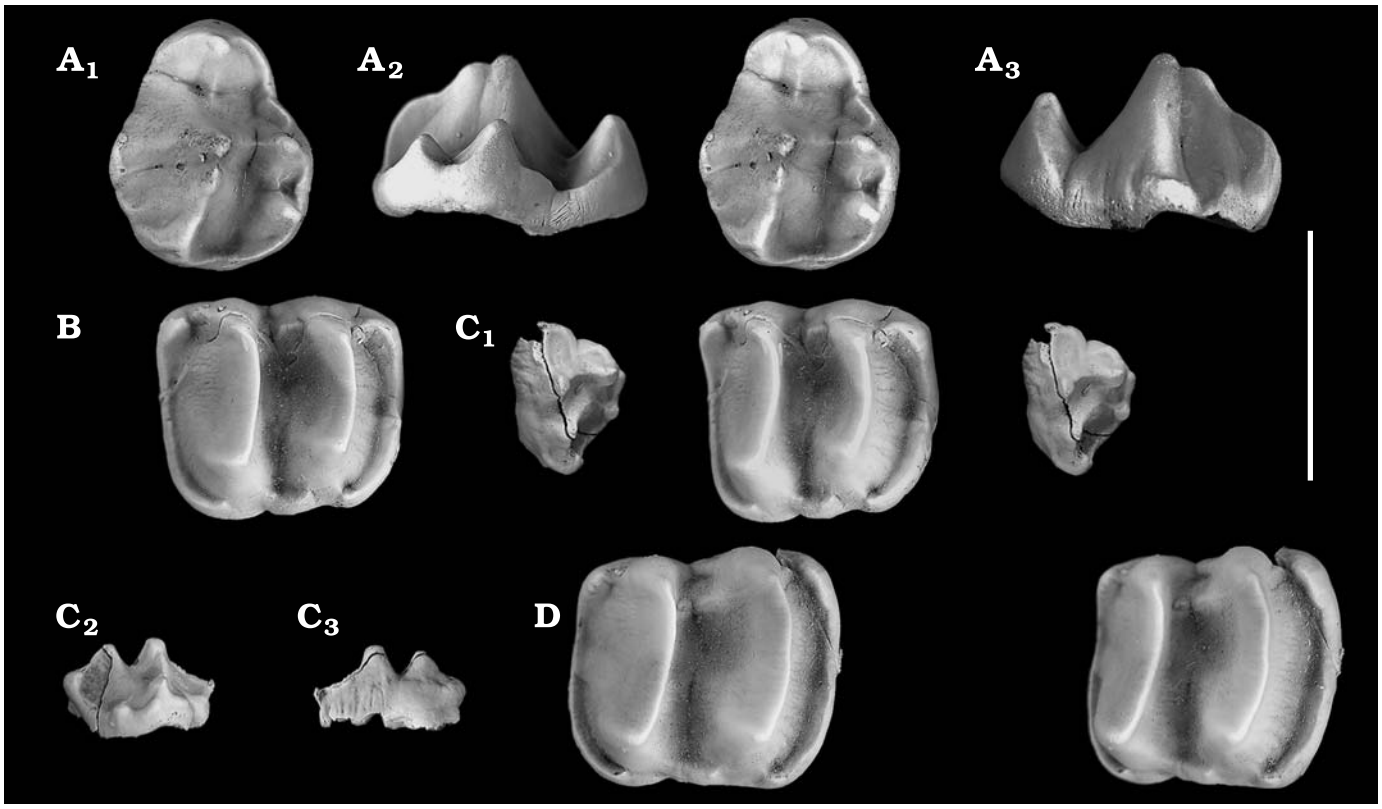

Fig. 3. Diprotodontid marsupial *Neohelos davidridei* sp. nov., holotype QM F40175, from the Middle Miocene Jaw Junction LF, Faunal Zone C, Riverlseigh World Heritage Area, Queensland, Australia. **A**. RP3; occlusal stereopair (A_1), lingual (A_2), and buccal (A_3) views. **B**. RM1; occlusal stereopair. **C**. Right deciduous P3; occlusal stereopair (C_1), lingual (C_2), and buccal (C_3) views. **D**. RM2; occlusal stereopair. Scale bar 20 mm.

Neohelos davidridei sp. nov.

Figs. 3, 4, Table 1.

2000 *Neohelos* sp. C; Murray et al. 2000b: 72–76, figs. 52–54.

Etymology: In honour of the late William David Lindsay Ride AM (1926–2011), former Director of the Western Australian Museum, Chief Research Scientist of CSIRO, explorer of remote Central Australia, brilliant vertebrate paleontologist, mammalogist, taxonomist and valued mentor to his students.

Holotype: QM F40175, partial tooth row consisting of an isolated right dP3, P3, M1–2 and maxilla fragments.

Type locality: Jaw Junction Site, Faunal Zone C deposits, Riversleigh World Heritage Area fossil deposit, Queensland, Australia.

Type horizon: The JJ Site is at the stratigraphically highest (201 m) level of the northern section of the Gag Plateau sequence (Creaser 1997). On the basis of stratigraphy and stage-of-evolution biocorrelation, the JJ Site is thought to be one of the youngest FZ C deposits and approximately Middle Miocene in age.

Referred specimens.—From JJ Site: QM F40174, Lm1 and dentary fragments; QM F40176, Lm2–3 and LM4; QM F40177, Ri1; QM F40178, RP3; QM F40179, Rm2; QM F40182, Rp3; QM F40180, partial Rm1; QM F40181, RM1 missing most of metaloph; QM F40186 (NTM P91168-2), RM3.

Diagnosis.—*Neohelos davidridei* differs from other species of *Neohelos* in the following combination of features: higher crowned; p3 lacking anterior crest with a gently sloping anterior protoconid face; p3 that lacks a distinct division between its anterior and posterior moieties; P3 with incipient division of the parametacone into its respective cusps; P3 parastyle larger and more separated from the parametacone base, resulting in a more elongate premolar overall. *Neohelos davidridei* differs from *Ne. solus* and *Ne. tirarensis* in having larger molars. *Neohelos davidridei* differs from *Ne. solus* in: having proportionately broader molars with less arcuate protolophs and less convex paracone and metacone buccal margins; lacking the posterolingual crest that ascends the metaloph on M1–2; having a continuous, arcuate lingual cingulum on M1; and in having a lower paralophid and broader protolophid on m1.

Description

Holotype.—*dP3* (Fig. 3): The deciduous P3 is a small, subtriangular tooth with four primary cusps including an anterior paracone, posterior metacone, anterolingual protocone and posterolingual hypocone. A possible fifth cusp, a weak parastyle, may have been situated at the anterior border of the tooth, however, this region is broken. The paracone is the tallest cusp, followed by the metacone, protocone and hypocone. The apices of the paracone and metacone are in line anteroposteriorly, just lingual to the midline of the tooth, and separated by a V-shaped valley. The protocone and hypocone are situated on the lingual margin, which is swollen and ovate—unlike the buccal margin, which is linear. Weak lingual crests extend from the apices of the paracone and metacone into the

http://dx.doi.org/10.4202/app.2012.0001

shallow longitudinal valley separating them from the protocone. A weak postmetacrista extends to the posterior tooth margin, becoming cuspate at this point. The posterolingual cingulum is weak and connects this posterior cuspule with a small hypocone. A buccal cingulum is absent. The anterior parastylar region is distinctly emarginated on the anterolingual crown base.

P3 (Fig. 3): P3 is a sub-ovate, quadritubercular tooth consisting of a large central parametacone, a well-developed anterior parastyle, a lingual protocone and a posterolingual hypocone. The parametacone is the tallest cusp, followed by the parastyle, protocone and hypocone. The protocone and hypocone are pyramidal in occlusal view. The premolar exhibits distinct anterior and posterior moieties and is widest across the protocone. The parametacone shows incipient differentiation into a respective paracone and metacone. The paracone apex is distinguished from that of the metacone by its greater height. Additionally, a shallow fissure extends down the buccal tooth margin from the point of division of the respective cusps. A lingual fissure is also present. The distinct paracone apex is connected to the blade-like apex of the metacone by a short ridge. The parametacone is pyramidal in occlusal view with distinct anterior, buccal and lingual faces. The large, erect parastyle is situated at the anterior tooth margin and separated from the parametacone by a relatively deep transverse valley. The lingual surfaces of the parametacone are steep and almost vertical. The buccal faces slope more gently towards the buccal tooth margin. A small anterolingual basin is bordered by the posterolingual base of the parastyle, the anterolingual base of the parametacone and the anterior base of the protocone. The apex of the parastyle lies directly anteriorly opposite the apex of the parametacone. A well-developed protocone lies opposite and slightly anterior to the parametacone apex on the lingual tooth margin. Two faint, transversely directed cristae from the apices of the parametacone and protocone meet in the longitudinal valley separating these cusps. A small hypocone lies posterior and slightly lingual to the protocone. A well-developed post-parametacrista extends posteriorly and slightly buccally to the posterior tooth margin and is continuous with the lingual and buccal cingula. The buccal cingulum curves anterobuccally around the base of the crown. A small mesostyle exists as a swelling on the buccal margin at a point opposite the parametacone. A continuous posterolingual cingulum extends from the postparametacrista in an anterolingual direction to the hypocone apex. It then travels into the valley between the hypocone and protocone, resulting in the formation of a deep basin, and continues up to the protocone apex and anteriorly into the anterolingual basin, and up to the parastyle apex. A slight swelling of the lingual cingulum at the anterolingual base of the protocone represents a small protostyle.

QM F40178 (Fig. 4), another RP3, is similar overall to QM F40175, except for the following differences: the protocone is taller with a broader lingual base; the incipient division of the parametacone is less distinct and the fissure extending down its buccal face is absent; the parastyle apex is more buccally positioned; and the posterobuccal cingulum and mesostyle are better developed.

M1 (Fig. 3): The M1 is relatively square in occlusal outline, although the metaloph is slightly wider than the protoloph. The tips of the lophs are slightly crescentic and overhang their bases anteriorly. The parastyle and metastyle are well developed, but positioned low on the crown. The parastyle is dominated by a distinct crescentic ridge that becomes continuous with the anterior cingulum. The metastyle is more distinctly cuspate than the parastyle and is continuous with the posterior cingulum. A short cleft separates the metastyle from the moderately developed postmetacrista. A weaker postparacrista extends down the posterobuccal face of the paracone, becoming more distinct at the buccal border of the transverse median valley. The transverse median valley is open buccally, yet closed lingually by a short, crescentic lingual cingulum. The anterior and posterior cingula are well developed, but not continuous with the lingual cingulum. Instead, they terminate at the anterolingual and posterolingual bases of the protocone and metaconule, respectively. The anterior cingulum becomes mildly cuspate midway along its length where it rises dorsally.

M2 (Fig. 3): M2 similar to M1, except that: it is larger; wider anteriorly than posteriorly with a corresponding wider protoloph; the parastyle and metastyle are reduced; the postparacrista and postmetacrista are absent; and the lingual cingulum is reduced and less arcuate.

Referred material.—*M3*: QM F40186, unworn enamel cap missing the posterolingual tooth corner including the metaconule. It is similar to the M2 of the holotype, except that: the metaloph is reduced both in height and width, resulting in a trapezoidal tooth outline; the protoloph is wider and more crescentic; and a metastyle is absent.

M4: QM F40176, unworn enamel cap similar to M3, except that: it is lower crowned; the metaloph is further reduced in both width and height and is more convex buccally; the parastyle, metastyle and posterior cingulum are absent; the lophs are less anteriorly overhanging; and the transverse median valley is wider and more open both buccally and lingually.

i1 (Fig. 4): QM F40177, a right i1, is heavily worn and missing its root. It is a deep (maximum depth 18.5 mm), broadly lanceolate tooth with a 5 mm section of dentine exposed from its medially curved tip to its posterior border. A series of longitudinal ridges cross the enamel medially. A fine ridge of enamel overhangs the exposed dentine dorsally. The maximum mediolateral thickness of the incisor is 11.0 mm.

p3 (Fig. 4): QM F40182, a right p3, is a large, sub-triangular, unworn tooth that tapers anteriorly. It is dominated by a single central cuspid, the protoconid (13.4 mm high). The anterior face of the protoconid slopes gently and evenly at an angle of 45° to the base of the crown. An anterior protoconid crest is absent. The posterior protoconid crest slopes steeply for 4 mm, then extends almost horizontally to the posterior tooth margin, becoming continuous with a well-defined arcuate posterolingual cingulum. A lingual, non-crested buttress extends vertically from the protoconid apex to the base

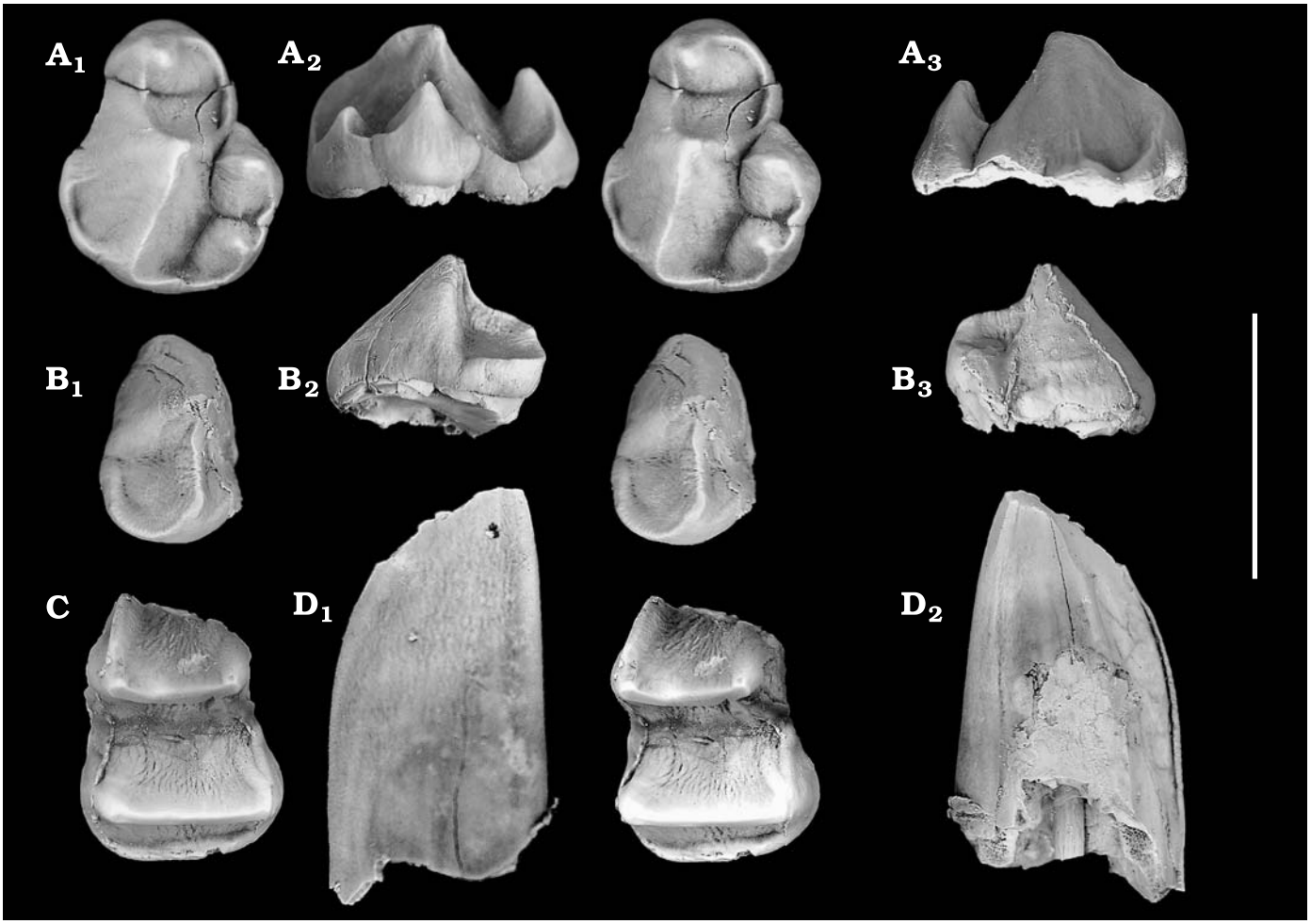

Fig. 4. Diprotodontid marsupial *Neohelos davidridei* sp. nov. referred material from the Middle Miocene Jaw Junction LF, Riversleigh World Heritage Area, Queensland, Australia. **A**. QM F40178, RP3; occlusal stereopair (A_1), lingual (A_2), and buccal (A_3) views. **B**. QM F40182, Rp3; occlusal stereopair (B_1), lingual (B_2), and buccal (B_3) views. **C**. QM F40174, Lm1; occlusal stereopair. **D**. QM F40177, Li1; lingual (D_1) and buccal (D_2) views. Scale bar 20 mm.

of the crown, defining the lingual fossa anteriorly. A weak posterobuccal cingulum exists as a swelling at the posterobuccal tooth corner and fades into the base of the crown. The lingual and buccal tooth margins curve gently from anterior to posterior. Consequently, there is no division of the tooth into anterior and posterior moieties.

m1: QM F40174 (Fig. 4), a left, nearly complete, subrectangular, unworn m1 that is missing its anterior border and enamel from the lingual face of the metaconid and buccal face of the protoconid. The protolophid is narrower (10.3 mm) than the hypolophid (12.9 mm) and slightly more crescentic. A strong, steep paralophid extends ventrally from the protoconid to the base of the crown. In QM F40180, which preserves the anterior tooth border, the paralophid is continuous with a short cingulum. A small pocket is formed between the steep anterior face of the protolophid and the anterior cingulum. A weaker anterobuccal cingulum curves around the base of the crown from its junction with the paralophid, but its extent cannot be determined. A weak premetacristd and prehypocristid fade down the anterior faces of their respective cuspids. A low, irregular posterior cingulum rises towards the tooth midline. The hypoconid is shorter than the entoconid. The transverse median valley is open lingually and buccally, and is V-shaped in lateral view.

m2: QM F40174 and QM F40179 are both left m2s. The m2 is a sub-rectangular tooth that is similar to m1, except for the following: it is larger overall; the paralophid is absent; the protolophid is wider than the metalophid; both lophids are more crescentic and the protolophid is more curved than the hypolophid; the transverse valley is broader, more open and U-shaped in lateral view; and the tips of the lophids overhang their bases slightly posteriorly.

m3–4: QM F40176, left unworn enamel caps of m3–4. m3 is similar to m2, except for the following: it is larger; the protolophid is wider; the transverse median valley is broader and U-shaped in lateral view. m4 is similar to m3, except for the following: the protolophid is wider but lower; the metalophid is reduced; and the anterior cingulum is less lingually extensive.

Geographic and stratigraphic range.—Middle Miocene; JJ Site, Riversleigh World Heritage Area, northwestern Queensland.

http://dx.doi.org/10.4202/app.2012.0001

Neohelos tirarensis Stirton, 1967

Fig. 5, Table 1.

Holotype: SAMP 13848, portion of a left P3 preserving the parametacone, protocone, and hypocone.

Type locality: Leaf Locality (UCMP Locality V6213), Kutjamarpu LF, Wipajiri Formation, Lake Ngapakaldi, South Australia (Stirton et al. 1967).

Type horizon: The Kutjamarpu LF is estimated to be Early Miocene in age (Archer et al. 1997; Megirian et al. 2010) on the basis of close faunal comparisons with local assemblages from Riversleigh.

Referred specimens.—From Leaf Locality, Lake Ngapakaldi, South Australia: AM F87625, RP3; AM F87626, LM2; AR456, M1; AR3340, I3; AR3358, I3; AR3459, RM2; SAM/UC465, RM1; UCMP 69977, LM1; UCMP 69978, RM2; UCMP 69979, m3. The following material is from the Riversleigh WHA, Queensland. From BC2 Site: QM F36321, LP3; QM F36322, C1; QM F36535, Lm1. From BR Site: QM F40163, LP3; QM F24137, left maxilla with M1–4. From BO Site: QM F40124 (NTM P91166-1), right maxilla, canine alveolus and P3; QM F40125 (NTM P91166-2), edentulous premaxilla; QM F40128 (NTM P91166-3), edentulous premaxilla; QM F40126 (NTM P91166-6), crushed braincase; QM F40127 (NTM P91166-7), Li1; QM F40028, Lm1. From CS Site: QM F40133, LP3; QM F40134, LM3; QM F40135, Rp3; QM F40136, RP3; QM F40137, RP3; QM F56235, Lp3; QM F40138, LM3–4; QM F40139, Lm1; QM F40140, left maxilla with M1–2; QM F40141, Rm1. From CR Site: QM F56236, left partial maxilla with P3 and anterior margin of M1. From Site D: CPC22558, RP3, M2; QM F41043, right dentary with i1, p3, m1–4; QM F41044, left dentary with i1, p3, m1–4. From DT Site: QM F56237, LP3. From Dunsinane Site: QML935, left maxilla with P3–M1–4 (still in matrix but with crowns exposed). From FT Site: QM F23157, partial right maxilla with P3, M1–4. From Inabeyance Site: QM F13088, palate with LP3–M1–3, RM2–4. From JJS Site: QM F40145, RP3; QM F40146, m3. From KCB Site: QM F56137, left partial maxilla with P3–M1; QM F56238, LP3; QM F30383, RM3; QM F30479, Lp3; QM F41200, left partial dentary with p3, m1–2. From MM Site: QM F40147, LM2; QM F40148, Lm3; QM F40149, LM3; QM F40150, LP3; QM F40151, right maxilla with P3, M1–3,M4. From NG Site: QM F40152, Lm3; QM F40153, RM3; QM F40154, Rm3; QM F12449, Rm1. From NP Site: QM F30868, Lm1. From Stick Beak Site: QM F56239, left partial M2, M3–4; QM F40130; right maxilla with P3–M1; QM F40173, right dentary fragment with p3–m1; QM F40131, LP3. From UBO Site: QM F40129 (NTM P91167-1), partial cranium with RP3, M1–4 and LM2–4. From Wang Site: QM F56240, Lm2. From WW Site: QM F40155, right partial dentary with p3, m1–4; QM F40156, RM3; QM F40157, left partial dentary with p3–m1; QM F56135, right partial maxilla with P3, M1–4 (M3 missing buccal protoloph). From WH Site: QM F56241, Rp3.

Revised diagnosis.—*Neohelos tirarensis* differs from *Ne. solus*: in having squarer, proportionately broader upper molars; in having a more consistently developed posterobuccal cingulum, mesostyle and transverse parametacone crest on P3; in having a weaker anterobuccal parametacone crest on P3; in having a more continuous lingual cingulum and better developed stylar cusps on M1; in lacking the posterolingual metaconule crest on M1; and in having a lower paracristid and higher protolophid on m1. *Neohelos tirarensis* differs from *Ne. stirtoni*: in being generally smaller; having a less bladed, more pyramidal parametacone on P3; and in having an upper canine. *Neohelos tirarensis* differs from *Ne. davidridei*: in being smaller and lower crowned; in having a smaller parastyle that is less separated from the base of the parametacone on P3; in lacking the incipiently divided parametacone on P3; in having less overhanging upper molar lophs; and in having a well-developed anterior protoconid crest on p3.

Description of referred material.—*P3*: Description is based on the additional material QM F56135 (Fig. 5), QM F56237, QM F56236, QM F56238, and QM F36321, and is compared with both the holotype (SAMP 13848) and AMF87625, an unworn P3 enamel cap from the type locality, originally figured and referred to *Ne. tirarensis* by Hand et al. (1993) and later described by Murray et al. (2000b).

QM F56238, a left P3 from the KCB Site, is similar in overall size to AMF87625, though narrower anteriorly across the parastyle. The parastyle is taller however, as is the protocone and hypocone. The anterior parametacone crest is less distinct in QM F56238, yet the buccal cingulum is more greatly developed and the mesostyle is distinctly cuspate. It is very similar to the holotype in the development of the protocone and hypocone, but differs in having a more bulbous mesostyle and a less distinct transverse parametacone crest.

QM F56137, a left P3, also from KCB, is slightly larger than the holotype, but similar in the development of the protocone, hypocone and transverse parametacone crest. It differs in having a weaker mesostyle that is more of a swelling of the posterobuccal cingulum than a distinct cusp. It differs from AMF87625 in being larger and more elongate as a result of a more greatly developed parastyle anteriorly. Its buccal margin is more linear owing to the reduced mesostyle and its retraction towards the posterobuccal cingulum. These same differences distinguish QM F56137 from QM F56238, also from KCB.

QM F56237, a left P3 from DT Site, is less elongate than AMF87625, with a better developed parastyle, protocone and hypocone. The mesostyle exists as a bulbous swelling on the buccal margin opposite the parametacone apex, similar to the condition in the holotype. Consequently, the occlusal outline of QM F56237 is more bulbous posterobuccally than AMF 87625. The anterolingual cingulum is less well developed and does not ascend the anterior base of the protocone as it does in AMF87625.

QM F56236, a left P3 from CR Site, is unworn and dominated by a very tall central parametacone. The protocone is well developed, whereas the hypocone, although distinct, is a swelling on the posterolingual cingulum, the apex of which is continuous with a posterior crest from the protocone. Conse-

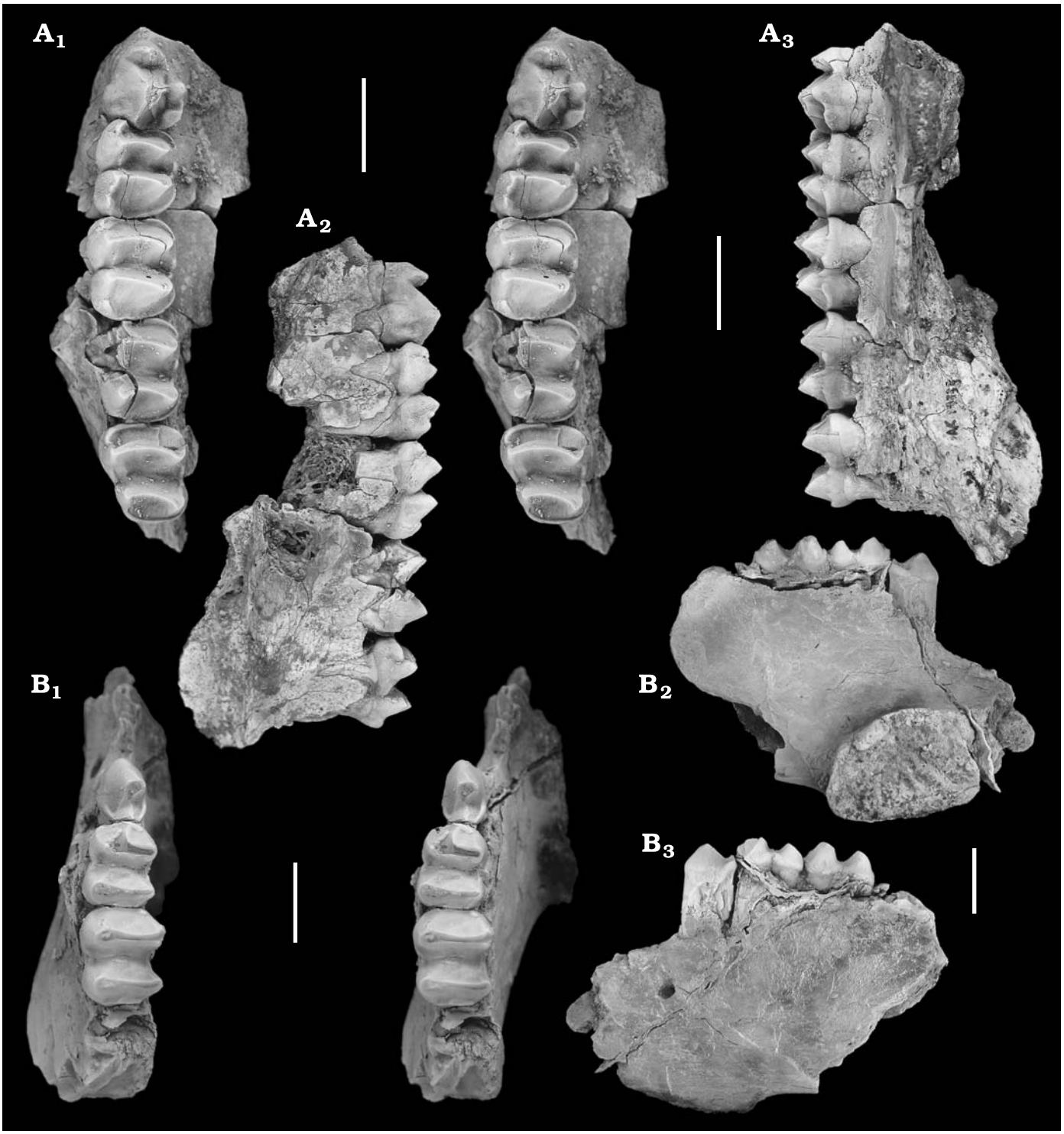

Fig. 5. Diprotodontid marsupial *Neohelos tirarensis* Stirton, 1967 material from the Riversleigh World Heritage Area, Queensland, Australia. **A**. QM F56135, partial right maxilla with P3–M4 from the Early Miocene Wayne's Wok LF; occlusal stereopair (A_1), buccal (A_2), and lingual (A_3) views. **B**. QMF41200, partial left dentary with p3–m2 from the Middle Miocene Keith's Chocky Block LF; occlusal stereopair (B_1), lingual (B_2), and buccal (B_3) views. Scale bars 20 mm.

quently, there is minimal separation between the bases of the protocone and hypocone, unlike that seen in the holotype and AMF87625. The parastyle is moderately tall and widely separated from the base of the parametacone which results in a more elongate tooth compared with AMF87625. The anterior parametacone crest is weak and fades out before reaching the valley between the parametacone and parastyle. The transverse link between the protocone and parametacone is well developed, as is the postparametacrista, which descends steeply to meet the parastyle of M1. Unlike in the holotype and

http://dx.doi.org/10.4202/app.2012.0001

AMF87625, a posterobuccal cingulum is absent, as is a mesostyle and, as a consequence, there is little emargination between the anterobuccal and posterobuccal tooth margins. QM F56236 is most similar to AR15119 (QM F40150), a left P3, from MM, referred by Murray et al. (2000b) to *Ne. tirarensis*.

The premolar of QM F56135 (Fig. 5), a right partial maxilla from WW Site, is "typically" *Ne. tirarensis*-like in occlusal outline and cusp development, and is strikingly similar to the holotype. It is also very similar to AMF87625, except that the parastyle and protocone are larger and the base of the hypocone is broader.

QM F36321, an unworn enamel cap from BC2 Site is slightly larger than AMF87625 and higher crowned. The parametacone is taller with a well-developed (albeit shorter) transverse crest. The parastyle is anteroposteriorly more elongate and larger overall. The hypocone is similarly developed to that in AMF87625, and the holotype, however, its apex is continuous with the posterolingual cingulum. A moderately cuspate, bulbous mesostyle lies opposite the parametacone apex and is the terminus of a well-developed posterobuccal cingulum.

Upper molars.—Description of the upper molars is based primarily on QM F56135 (Fig. 5), a right partial maxilla with P3, M1–4.

M1: The M1 is slightly larger than the paratype UCMP 69977 and most similar in morphology to the M1 of QM F40151, a right maxilla described by Murray et al. (2000b). As in QM F40151, the protoloph is shorter than the metaloph and both the parastyle and metastyle are well developed, resulting in a more trapezoidal outline to the crown. This feature is further emphasized in QM F56135 owing to a larger, more cuspate metastyle that connects the postmetacrista to the posterior cingulum. The anterior, lingual and posterior cingula are moderately developed, while a buccal cingulum is absent. In lateral view, the median transverse valley is broadly V-shaped. There is a large degree of interdental contact between M1 and P3, with the postparametacrista of P3 becoming almost continuous with the parastyle of M1. In QM F56138 which is a smaller tooth overall, the metastyle is weaker and the postmetacrista is lower than in QM F56135.

M2: The M2 of QM F56135 is similar to M1 but larger, with a wider protoloph than metaloph. The parastyle and metastyle are reduced and the postmetacrista is weak and not continuous with the posterior cingulum. It is very similar in size and morphology to AMF87626, a right M2 figured by Hand et al. (1993) and described by Murray et al. (2000b), from the Leaf Locality.

M3: The M3 of QM F56135 is missing the buccal margin of the protoloph, but, overall, appears to be narrower and more elongate than M2. The metastyle is further reduced, as is the metaloph.

M4: Similar to M3, but with the metaloph is further reduced and more crescentic. The parastyle is smaller but distinct, while the metastyle is absent.

Lower dentition.—*p3*: Additional p3s referred to *Ne. tirarensis* include: QM F56235, a left p3 (CS); QM F56241, a right p3 (WH); QM F30479, left p3 (KCB); and QM F41200 (Fig. 5B), a left partial dentary with p3, m1–2 (KCB). Comparisons of the lower premolar are made with QM F40135 (AR10641) from CS, which was described (but incorrectly numbered) as AR10841 by Murray et al. (2000b: 20, fig. 17), and QM F40155, a right dentary with p3, m1–4, described by Murray et al. (2000b: 22, fig. 19).

QM F56235 differs from QM F40135 and QM F40155 in being smaller, and in having: steeper anterior and posterior protocristids; a better developed lingual cingulum and, consequently, a deeper lingual fossa. QM F30479 is also smaller than QM F56235 and QM F40135, and has a more distinct lingual cingulum and deeper lingual fossa. However, the anterior protocristid is less steep and the posterior protocristid is less convex.

QM F56241, a Rp3 from the WH LF, is moderately worn on the protoconid and missing the enamel from the posterolingual tooth corner. It is smaller overall than QM F40155 and slightly less elongate than QM F40135. In differs from QM F40155 in having a weaker, less anteriorly extensive posterobuccal cingulum, although the latter is more strongly developed than in QM F40135. It differs further from QM F40135 in having a less steeply sloping anterior protoconid face and weaker anterior protoconid crest.

QM F41200 (Fig. 5) is the longest recorded *Ne. tirarensis* p3 (13.4 mm), yet is not as broad as QM F40155 owing to a linear, less bulbous posterobuccal tooth margin. The tooth is extremely worn, so that the height of the protoconid and the relative steepness of the posterior protocristid cannot be determined. The lingual cingulum is well developed and the lingual fossa is deep, but narrow.

m1: The m1 of QM F41200 (Fig. 5) is less elongate than QM F40155 (16.4 mm versus 17.4 mm), but far broader both anteriorly (12.6 mm versus 10.8 mm) and posteriorly (13.3 mm versus 12.2 mm). The reduced length is the result of a blunt, poorly developed paralophid and a far rounder anterior tooth margin than is the case in QM F40155. Other differences include a wider protolophid and less difference in the width of the protolophid compared with the hypolophid. QM F40028 (a left m1 from BO Site) exhibits the more characteristic well-developed paralophid as seen in QM F40155, yet is proportionately smaller overall; however, it is comparable in size to the Site D specimens QM F41043–44 described by Murray et al. (AR1685–86 in Murray et al. 2000b: 22, fig. 18).

m2: The m2 of QM F41200 (Fig. 5) is similar to m1 but wider anteriorly and posteriorly, with broadly rounded lingual and buccal bases of the lophids. The protolophid is wider than the hypolophid and the paralophid is absent. The interlophid valley is broadly V-shaped in occlusal view. It is similar to the m2 of QM F40155, yet with a broader protolophid and more linear, parallel arrangement of the lophids.

m3: QM F30383 is an isolated, unworn right m3 from KCB. It is deemed an M_3 owing to its size, but it is possible that it is a large m2. The tooth is high crowned with a

protolophid that is taller than the hypolophid. In lateral view, the crests of the lophids curve posteriorly. There are a weak buccal and lingual cingula positioned low on the crown. The apex of the protoconid is bulbous and a weak, short preprotocristid is present. The anterior cingulum is linear and short. The posterior cingulum is crescentic and elevated on the buccal side of its midline.

Dentary: QM F41200 (Fig. 5), a partial left dentary from KCB, retains only a short section of the horizontal ramus including the posterior border of the symphysis and the mental foramen. The dentary is deep 63.4 mm (measured below the anterior root of m1) and robust compared with QM F40155 (45 mm deep). The symphysis is unfused, broad (27.6 mm compared with 21.6 mm in QM F40155) and ovate along its posterior border, which extends to a point level with the anterior root of m1. The mental foramen (4 mm diameter) lies 1 mm anterior to the root of p3, and approximately 11 mm ventral to the diastemal crest (however, this area is poorly preserved). The sublingual fossa is shallow and narrow. A shallow, irregular genial pit lies at the posteroventral surface of the symphysis.

Remarks.—Extended descriptions and figures of the following referred material can be found in Murray et al. (2000b: 11-31): AR16492 (QM F40151), QM F13088, CPC22558, AR9947 (QM F40133), AR10726 (QM F40137), AR10362 (QM F40134), AR12120 (QM F40138), AR17291 (QM F40153), NTM P91167-1 (QM F40129), QM F24137, AR10641 (QM F40135), AR16787 (QM F40157), AR10458 (QM F40155), AR1685-6 (QM F41043-44), QM F12449, AR14393 (QM F40146), AR13795 (QM F40130), NTM P91166-2 (QM F40125), NTM P91166-1 (QM F40124), NTM P91166-7 (QM F40127), NTM P91166-6 (QM F40126).

A reanalysis by Black (2010) of the specimens NTM P-91171-2 (left P3 fragment and LM2) and NTM P91171-4 (Rm4), both from 300BR Site, and referred to *Ne. tirarensis* by Murray et al. (2000a), suggests they should be referred to *Ngapakaldia bonythoni*. The P3 fragment, regarded by Murray et al. (2000b) to be a LP3 parastyle of *Ne. tirarensis* is in fact a LP3 protocone of *Ng. bonythoni*. Further, the M2 and m4 are indistinguishable from *Ng. bonythoni* material from Riversleigh. Specimens NTM P91171-5 (LI1), NTM P91171-6 (RI3) and NTM P942-1 (M4), also from 300BR Site, have not been examined, and hence are not included in this study.

Geographic and stratigraphic range.—Early Miocene Kutjamarpu LF of the Wipajiri Formation, Lake Ngapakaldi, South Australia; Late Oligocene Kangaroo Well LF of the Ulta Limestone, Northern Territory; and numerous Late Oligocene to Middle Miocene deposits (FZ A–C) of the Riversleigh World Heritage Area, northwestern Queensland, Australia.

Neohelos stirtoni Murray, Megirian, Rich, Plane, and Vickers-Rich, 2000a

Fig. 6, Table 1.

Neohelos sp. B; Murray et al. 2000b: 38–72, figs. 29–51.

Holotype: CPC 22200, cranium with left and right P3, M1–4; missing part of right squamosal, parietal, zygomatic arch and left and right I2–3.

Type locality: Small Hills Locality, 26 km east southeast of Camfield Station Homestead, Bullock Creek, Northern Territory (approx. Latitude 17°07' S, Longitude 131°31' E).

Type horizon: On the basis of stage-of-evolution biocorrelation, the limestones of the Camfield Beds are believed to be Moddle Miocene in age (Archer et al. 1997; Murray et al. 2000a).

Additional material.—To the referred material listed in Murray et al. (2000a), we add the following Riversleigh specimens. From Gag Site: QM F40165, right maxilla with P3, M1–3; QM F40168, LP3; QM F40166, M1. From HH Site: QM F40167, LP3; QM F40170, Rm3; QM F40169, Rp3. From GS Site: QM F40117, left dentary fragment with m3 and protolophid of m4.

Revised diagnosis.—*Neohelos stirtoni* differs from *Ne. tirarensis* and *Ne. solus* in the following combination of features: larger; higher crowned dentition; bladed parametacone on P3; distinct, posteriorly increasing molar gradient; canine absent. *Neohelos stirtoni* differs from *Ne. solus* in having broader, squarer molars with less arcuate protolophs and less convex paracone and metacone buccal margins; in lacking the posterolingual crest that ascends the metaloph on M1–2; in having a continuous, arcuate lingual cingulum on M1 and in having a lower paralophid and broader protolophid on m1. *Neohelos stirtoni* differs from *Ne. davidridei* in: having a stronger anterior protoconid crest and associated cuspule on p3; having a proportionately less elongate P3; and in lacking an incipiently divided parametacone on P3.

Description

Upper dentition.—Description of the upper dentition is primarily based on QM F40165 (Fig. 6), a right partial maxilla with P3, M1–3. The dentition is generally unworn, except for slight wear on the parametacone and protocone of P3, the parastyle of M1 and the anterior faces of the lophs on M1–2.

P3: P3 with four cusps: a large anterior parastyle; a tall, central parametacone; a moderate lingual protocone; and a small posterolingual hypocone. The P3 is relatively small (17.1 mm in length), but falls within the size range displayed by the Bullock Creek *Ne. stirtoni* material (15.1–20.4 mm, mean 18.2 mm) found by Murray et al. (2000a). The parastyle is erect and widely separated from the base of the parametacone. A swelling exists at the buccal base of the crown opposite the parametacone, but a distinct mesostyle is absent, as is a posterobuccal cingulum. There is a strong lingual emargination between the bases of the parastyle and protocone. In many respects, the P3 of QM F40165 shows a similar development of features to the premolar figured by Murray et al. (2000a: fig. 28C). QM F40168, a partially encrypted LP3 also from Gag Site, is slightly longer (17.5 mm) and much broader (16.1 mm) than QM F40165, and differs in the following features: the anterior parastylar border is gently rounded (rather than pointed as in QM F40165), as is the protocone base; the hypocone is a small swelling of the

http://dx.doi.org/10.4202/app.2012.0001

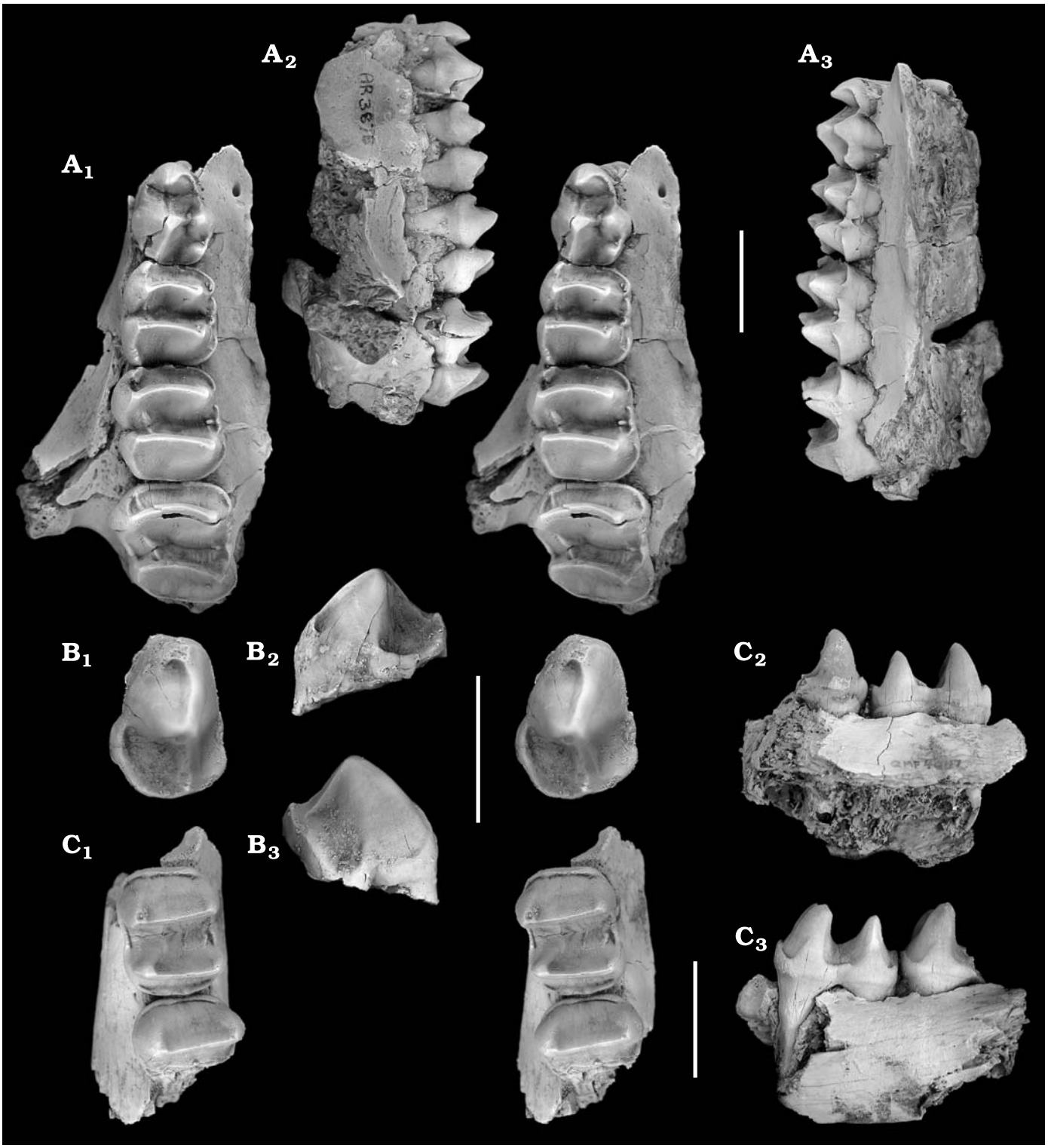

Fig. 6. Diprotodontid marsupial *Neohelos stirtoni* Murray, Megirian, Rich, Plane, and Vickers-Rich, 2000a, material from Middle Miocene deposits of the Riversleigh World Heritage Area, Queensland, Australia. **A**. QM F40165, partial right maxilla with P3–M3 from the Dwornamor LF (Gag Site); occlusal stereopair (A_1), buccal (A_2), and lingual (A_3) views. **B**. QM F40169, right p3 from the Henk's Hollow LF; occlusal stereopair (B_1), lingual (B_2), and buccal (B_3) views. **C**. QMF40117, left dentary fragment with m3 and protolophid of m4, from the Golden Steph LF; occlusal stereopair (C_1), lingual (C_2), and buccal (C_3) views. Scale bars 20 mm.

posterolingual cingulum, rather than a distinct cusp; and the mesostyle and posterobuccal cingulum are better developed and the mesostyle is distinctly cuspate.

M1–3: These molars are similar morphologically to specimens of *Ne. stirtoni* from Bullock Creek and, although small (e.g., M1 length 17.8 mm), fall within the size range for that

sample (17.2–21.7 mm). There is a distinct, posteriorly increasing molar gradient compared to *Ne. tirarensis*.

Lower dentition.—*p3*: QM F40169 (Fig. 6), a right p3, is a sub-ovate, anteriorly tapering tooth. There is slight wear on the protoconid apex, which is situated just posterior to the midline of the crown. A weak crest extends anteroventrally to approximately three quarters of the distance to the base of the crown, where it becomes weakly cuspate. It then curves lingually, forming a shallow anterior fossa between it and the base of the protoconid. A posterior protocristid bifurcates at the posterior tooth border into a well-developed posterolingual cingulum and a weaker posterobuccal cingulum. The lingual fossa is well defined by the postprotocristid buccally, the posterolingual cingulum, and a vertical buttress of the protoconid anteriorly.

m2: QM F40170, a right m2 from the HH LF is a large, sub-rectangular molar with a linear protolophid and slightly curved and obliquely offset hypolophid. The protolophid is slightly narrower and taller than the hypolophid. Both the anterior and posterior cingula are well developed but positioned low on the crown, rising towards the midline. The transverse valley is open buccally and lingually, and is U-shaped in lateral view.

m3–4: Description is based on QM F40117 (Fig. 6), a left dentary fragment with m3 and the protolophid of m4, from the GS LF. The m3 is similar to QM F40170 but larger, and the hypolophid is more obliquely offset with respect to the protolophid. The tip of the protolophid slightly overhangs its base posteriorly. The m4 is similar to m3, except that the protolophid is wider and taller buccally.

Remarks.—Murray et al. (2000b) referred specimens AR 13791 (QM F40172), a partial right dentary with m2–4 and AR13969 (QM F40173), a partial right dentary with p3–m1, both from SB Site, to *Neohelos* sp. B (= *Neohelos stirtoni*). A reappraisal of this material suggests QM F40172 is more appropriately assigned to *Ngapakaldia bonythoni* (Black 2010) and QM F40173 to *Ne. tirarensis*. Murray et al. (2000b: 65) note that the molar dimensions of AR13791 and QM F40173 are similar to those of *Bematherium* (synonymized with *Ng. bonythoni*; see Black 2010), but differ in having a well-developed paralophid crest on m1. This is true of QM F40173, which is unquestionably *Neohelos*. However, QM F40172 does not preserve an m1, but does retain the alveoli of the anterior and posterior root of p3, which suggests that the p3 was approximately 9.8 mm in length—dimensions that fall within the range of *Ng. bonythoni* (9.0–10.8 mm), but not *Ne. stirtoni* (11.5–17.9 mm). In terms of both the morphology of the dentary and dentition and molar dimensions, QM F40172 is most similar to specimens of *Ng. bonythoni*, which are common in Riversleigh's FZ A deposits, including SB, WH, Jeanette's Amphitheatre and Hiatus sites (Black 2010).

In regard to QM F40173, the lower premolar lacks the small anterior cuspid, the sharp anterior blade of the protoconid and the anterolingual fossa, which are characteristic of *Ne. stirtoni* lower premolars. In terms of both size and morphology, it is most similar to *Ne. tirarensis* material from Riversleigh's CS Site.

Geographic and stratigraphic range.—Middle Miocene; Bullock Creek LF, Camfield Beds, Northern Territory, and several FZ C deposits of the Riversleigh World Heritage Area, northwestern Queensland, Australia.

Discussion

The genus *Neohelos* was originally described by Stirton (1967) on the basis of five isolated teeth from the Wipajiri Formation, Lake Ngapakaldi, South Australia. Hand et al. (1993) referred a further two specimens from the type locality (P3 and M2) to the type and only species, *Neohelos tirarensis*. Since that time, additional, more complete material of *Neohelos tirarensis*, as well as several new species, has been recovered from the Riversleigh WHA, north-western Queensland and Bullock Creek, Northern Territory (Murray et al. 2000a, b). This material, consisting of hundreds of specimens, including complete crania and postcranial material from Bullock Creek, formed the basis of a joint 1996 study that was submitted for publication in *Records of the Queen Victoria Museum* (Launceston) by P. Murray, D. Megirian, T.H. Rich, M. Plane, M. Archer, S.J. Hand, P. Vickers-Rich, and K. Black, in which three new *Neohelos* species were recognized. For reasons outlined by Murray et al. (2000a) the manuscript was withdrawn from publication and later made available as an unpublished Report of the Museums and Art Galleries of the Northern Territory (MAGNT Report 6; Murray et al. 2000b hereafter). Although material was described in the report as *Neohelos* sp. A, sp. B, and sp. C, no new species names were given and holotypes were not formally identified. A substantial portion of Murray et al. (2000b) was subsequently extracted and published by Murray et al. (2000a), who formally named *Neohelos* sp. B as *Ne. stirtoni*. However, only material from the Bullock Creek LF, Northern Territory was included in Murray et al. (2000a), leaving all Riversleigh materials without taxonomic assignment and hence revision of the genus incomplete.

A preliminary analysis of the diversity and distribution of diprotodontoid material from Riversleigh by Black (1997) recognized four *Neohelos* species: *Neohelos* sp. nov. 1 (a small, plesiomorphic form); *Ne. tirarensis* (a medium-sized form); *Neohelos* sp. nov. 2 (a larger, derived form = *Ne. stirtoni*); and *Neohelos* sp. nov. 3 (the largest and most highly derived form). At the time, *Neohelos* sp. nov. 1 included material from Riversleigh's FZ A deposits (e.g., BO, Site D, BR, SB) and COA Site, as well as material previously identified by Hand et al. (1993) as *Nimbadon scottorrorum* from FT Site, but subsequently referred to *Neohelos* by Black and Archer (1997b).

Since publication of Black (1997), and prior to completion of Murray et al. (2000b), analysis of new *Neohelos* mate-

http://dx.doi.org/10.4202/app.2012.0001

Table 2. *Neohelos solus* sp. nov. univariate statistics (using left side only). Abbreviations: AW, anterior width; CV, coefficient of variation; L, length; Max, maximum value; Min, minimum value; N, sample size; PW, posterior width; SD, standard deviation; SE, standard error; W, width.

	N	Min	Max	Mean	SE	SD	Median	CV
P3L	5	14.2	14.6	14.4	0.0	0.2	14.3	1.1
P3W	5	12.0	13.4	12.7	0.1	0.5	12.6	4.2
M1L	10	15.4	17.1	16.4	0.1	0.6	16.4	3.6
M1AW	10	12.7	14.5	13.7	0.1	0.5	13.8	3.7
M1PW	10	13.2	14.8	13.9	0.1	0.5	14.0	3.4
M2L	8	16.7	18.7	17.3	0.1	0.6	17.1	3.6
M2AW	7	14.3	15.9	15.3	0.1	0.6	15.5	4.2
M2PW	8	14.0	15.6	14.5	0.1	0.6	14.4	4.0
M3L	9	17.2	18.7	17.8	0.1	0.5	17.9	3.0
M3AW	8	15.0	16.4	15.7	0.1	0.5	15.5	3.3
M3PW	9	13.1	14.4	13.8	0.1	0.4	13.7	2.8
M4L	2	16.2	19.1	17.7	0.4	2.1	17.7	11.6
M4AW	2	13.9	16.9	15.4	0.4	2.1	15.4	13.8
M4PW	2	11.4	13.4	12.4	0.3	1.4	12.4	11.4
p3W	8	10.5	14.1	12.3	0.2	1.2	12.1	9.8
p3L	8	7.0	9.4	8.3	0.2	0.8	8.4	9.8
m1L	7	14.7	17.1	15.8	0.2	1.0	15.7	6.1
m1AW	7	8.8	10.7	9.8	0.1	0.6	10.0	6.5
m1PW	7	10.3	11.7	10.9	0.1	0.7	10.8	6.0
m2L	3	17.0	17.6	17.2	0.1	0.3	17.1	1.9
m2AW	3	11.8	12.7	12.2	0.1	0.5	12.1	3.8
m2PW	3	11.5	12.5	12.0	0.1	0.5	12.0	4.2
m3L	6	17.2	18.8	17.8	0.1	0.6	17.7	3.4
m3AW	6	12.2	13.9	13.2	0.1	0.7	13.4	5.1
m3PW	6	12.0	12.8	12.4	0.1	0.4	12.5	3.0
m4L	1	18.5	18.5	18.5	0.0	0.0	18.5	0.0
m4AW	1	13.1	13.1	13.1	0.0	0.0	13.1	0.0
m4PW	1	12.0	12.0	12.0	0.0	0.0	12.0	0.0

rial from Riversleigh has served to blur the boundaries of distinction between the small *Neohelos* species from Riversleigh's FZ A deposits and the characteristic *Ne. tirarensis* from Riversleigh's FZ B deposits. This led Murray et al. (2000b) to interpret the Riversleigh FZ A *Neohelos* material as chronomorphs of the species *Ne. tirarensis*. Further, the discovery of a partial maxilla (QM F30878, Fig. 1) preserving P3–M3 from COA Site, highlighted some key morphological differences between the COA sample and the rest of the *Neohelos* material previously deemed to represent *Neohelos* sp. nov. 1. Consequently, Murray et al. (2000b) recognized four species of *Neohelos*: *Neohelos* sp. A (comprising the COA sample); *Ne. tirarensis* (which includes all the *Neohelos* material from FZs A and B); *Neohelos* sp. B (subsequently named *Ne. stirtoni* by Murray et al. 2000a); and *Neohelos* sp. C (*Neohelos* sp. nov. 3 of Black 1997). Further, they suggested that the "*Nimbadon" scottorrorum* type specimen may represent a fifth species of *Neohelos*, based on the unique development of the postcingulum on the metaconule of the upper molars.

Here, we recognize four species of *Neohelos*: *Ne. tirarensis*, *Ne. solus* sp. nov. (*Neohelos* sp. A of Murray et al. 2000a), *Ne. stirtoni*, and *Ne. davidridei* sp. nov. (*Neohelos* sp. C of Murray et al. 2000b). These species are essentially those defined by Murray et al. (2000b), with the exception that *Ne. scottorrorum* is assigned to *Ne. tirarensis*. *Neohelos solus* is the most plesiomorphic member of the genus, followed by *Ne. tirarensis*, with *Ne. stirtoni* and *Ne. davidridei* forming a derived sister-group. *Neohelos davidridei* is further derived with respect to *Ne. stirtoni* on the basis of the incipient division of the parametacone of P3.

New material for the type species, *Ne. tirarensis*, has been recovered from eight Riversleigh sites spanning FZ A (e.g., WH), through FZ B (e.g., DT, NP and CR) and FZ C (Wang, BC 2, and KCB). *Neohelos tirarensis* is now, temporally and geographically, the most wide-ranging species of the genus, having been recorded in the Late Oligocene Kangaroo Well LF of the Northern Territory, the Early to Middle Miocene Kutjamarpu LF of South Australia, and twenty Late Oligocene to Middle Miocene deposits at Riversleigh. Coefficients of variation of dental dimensions (Table 3) suggest this material generally falls within the level expected for a single, mixed-sex population (Simpson et al. 1960). Morphological variation, however, particularly in the development of cusps, crests and cingula of P3, is high (Table 1). Black and Hand (2010) found a similarly high degree of variation in premolar morphology in the zygomaturine *Nimbadon lavarackorum*, as did Price (2008) and Price and Sobbe (2010) for the diprotodontine *Diprotodon optatum*.

Despite this wide morphological, temporal and geographic range, *Ne. tirarensis* is still regarded to be a useful species for stage-of-evolution biocorrelation. The additional material described in this paper supports the chronological morphocline proposed by Murray et al. (2000a, b) from *Ne. tirarensis* through *Ne. stirtoni*, to *Ne. davidridei*. This morphocline is reflected in a gradual change in dental morphology accompanied by an overall increase in size (Fig. 7). A similar chronological morphocline was identified by Price and Piper (2009) within the late Cenozoic diprotodontid genera *Euryzygoma* and *Diprotodon* (e.g., from *E. dunense* through *D.* ?*optatum* to *D. optatum*).

Superficially, Table 1 may suggest a high degree of random morphological variation in the development of structures on P3 across species of *Neohelos*, but some general trends are evident. *Neohelos tirarensis* premolars from FZ A tend to be smaller in overall size (i.e., <15 mm in length), have small parastyles, small hypocones and weakly developed transverse parametacone crests. *Neohelos tirarensis* premolars from FZ B–C deposits are generally moderate in size (i.e., 15–17 mm in length), have moderately developed parastyles, small to moderate hypocones and generally stronger transverse parametacone crests. *Neohelos stirtoni* specimens are larger still (i.e., 17–19 mm in length), higher crowned, with moderately developed parastyles, and a weakening of the transverse parametacone crest. The morphocline culminates in *Ne. davidridei* (P3 length > 20 mm), which displays a large parastyle on P3,

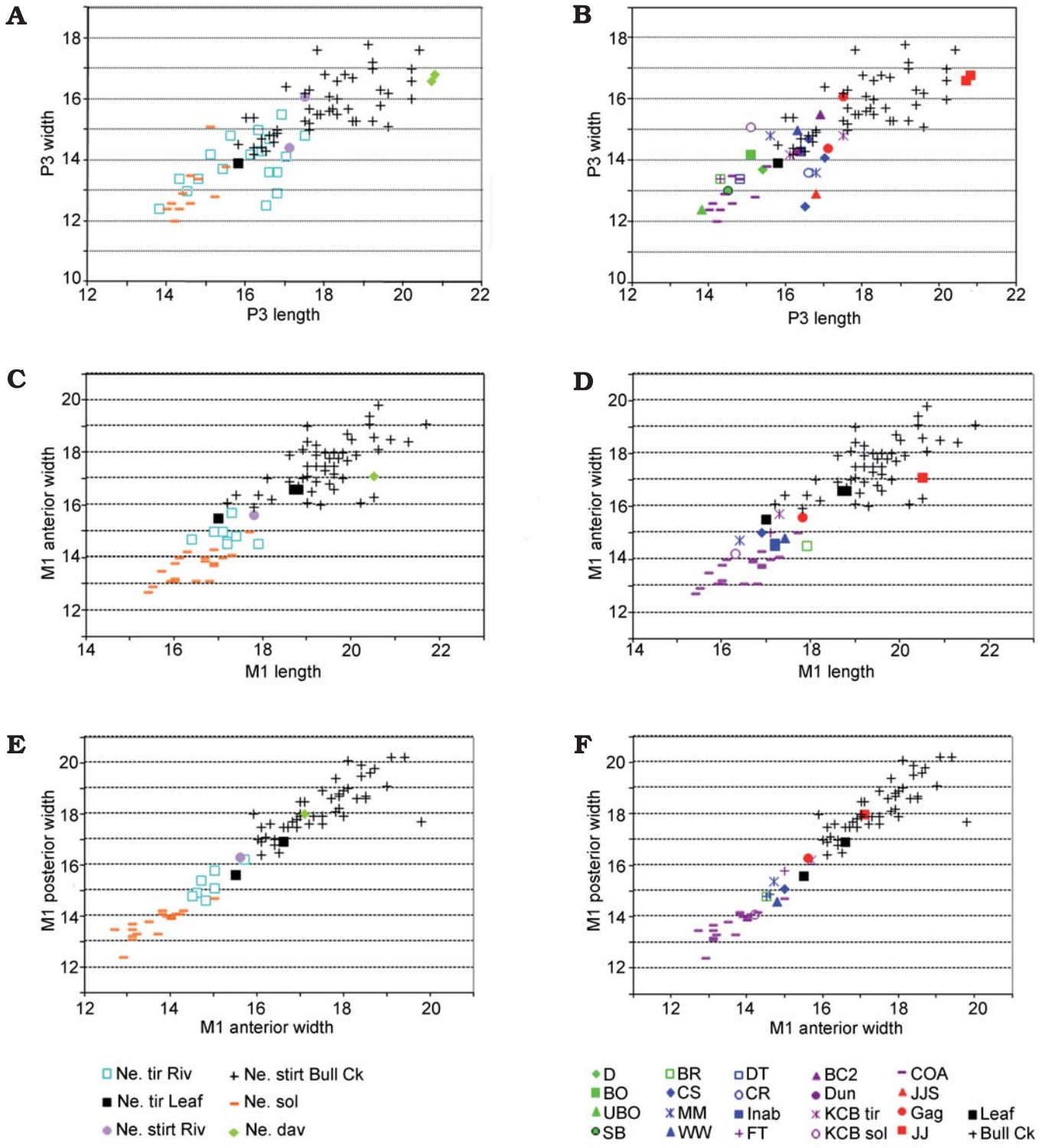

Fig. 7. Scatter plots of *Neohelos* P3 and M1 dimensions (in mm) from the Riversleigh World Heritage Area, Queensland, the Leaf Locality, South Australia, and the Bullock Creek LF, Northern Territory. **A**. P3 length versus width segregated by species. **B**. P3 length versus width segregated by site and faunal zone. **C**. M1 length versus anterior width segregated by species. **D**. M1 length versus anterior width segregated by site and faunal zone. **E**. M1 anterior width versus posterior width segregated by species. **F**. M1 anterior width versus posterior width segregated by site and faunal zone. Abbreviations: Bull, Bullock Creek; dav, *davidridei*; Leaf, Leaf Locality; Ne, *Neohelos*; tir, *tirarensis*; Riv, Riversleigh; sol, *solus*; stirt, *stirtoni*. Riversleigh site abbreviations: BC2, Black Coffee 2; BO, Burnt Offering; BR, Bone Reef; COA, Cleft Of Ages; D, Site D; CR, Creaser's Ramparts; CS, Camel Sputum; DT, Dirk's Towers; Dun, Dunsinane; FT, Fig Tree; Inab, Inabeyance; JJ, Jaw Junction; JJS, Jim's Jaw; KCB, Keith's Chocky Block; MM, Mike's Menagerie; SB, Sticky Beak; UBO, Upper Burnt Offering; WW, Wayne's Wok. Measurements from Table A (Appendix 2). Colors in graphs B, D, and F denote Riversleigh faunal zones: Faunal Zone A (Late Oligocene), green; Faunal Zone B (Early Miocene), blue; Faunal Zone C (Middle Miocene), red; uncertain age, purple; non-Riversleigh sites, black.

http://dx.doi.org/10.4202/app.2012.0001

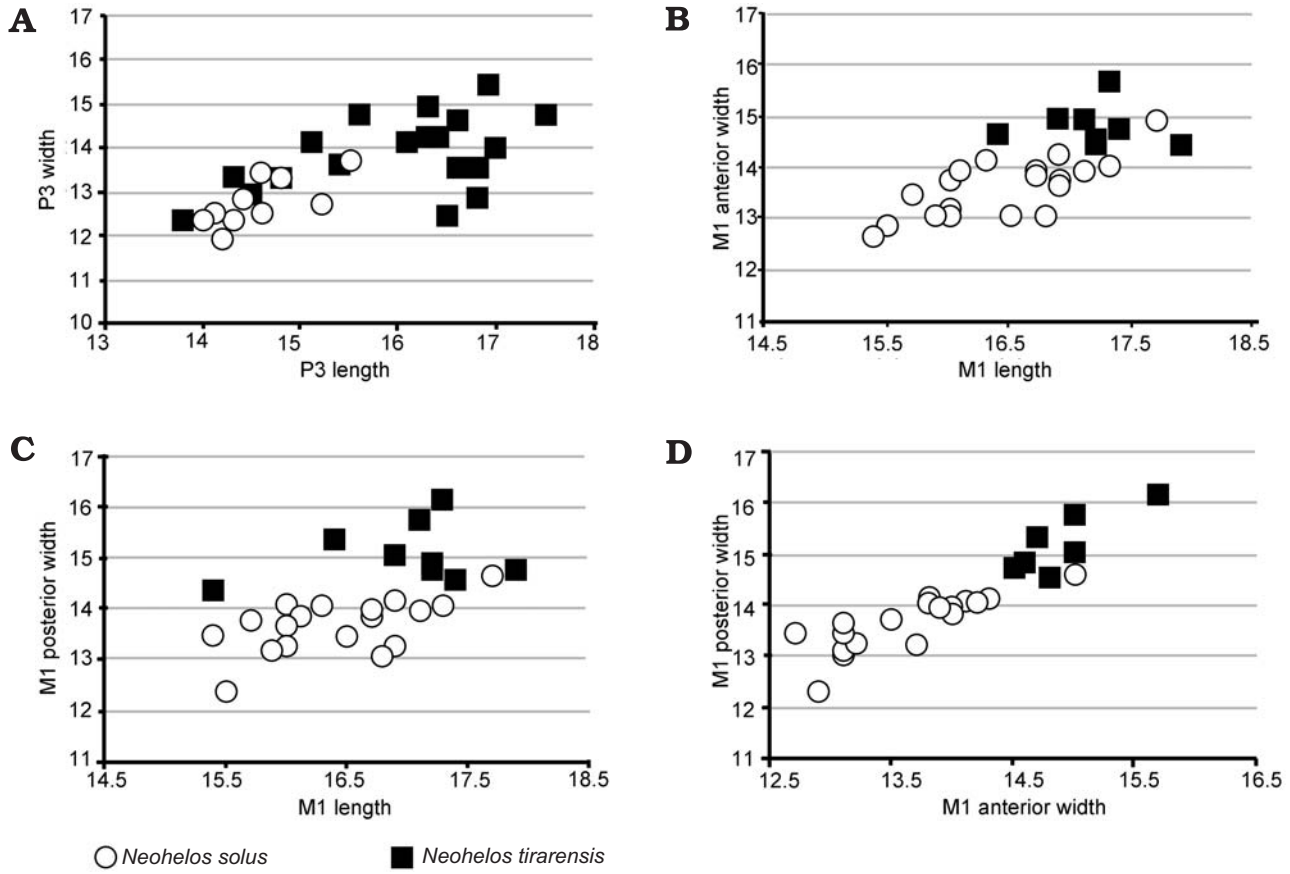

Fig. 8. Comparison of *Neohelos tirarensis* and *Neohelos solus* sp. nov. P3 and M1 dimensions (in mm). **A**. P3 length versus width. **B**. M1 length versus anterior width. **C**. M1 length versus posterior width. **D**. M1 anterior width versus posterior width.

an incipiently divided parametacone, a moderately developed hypocone and a further weakening or absence of the transverse parametacone crest.

Comparison of Fig. 7A and B indicates that *Ne. tirarensis* is the predominant species in FZ A and FZ B, with smaller chronomorphs of the species occurring in the older FZ A deposits (e.g., D, BO, UBO, SB, and BR) and larger, more "typical" *Ne. tirarensis* material present in FZ B deposits (e.g., CS, MM, WW, Inab). *Neohelos stirtoni* material from Riversleigh's FZ C deposits falls within the lower end of the size range recorded for the Bullock Creek population. On the basis of P3 dimensions, there is a large overlap between the *Ne. stirtoni* and *Ne. tirarensis* samples from Bullock Creek and Riversleigh, respectively (Fig. 7A). Analysis of molar dimensions, however, shows minimal overlap with a more pronounced distinction between the species (Fig. 7C–F), and suggests that molars may be more useful in determining the relative position of a *Neohelos* sample on the chronological morphocline. *Neohelos davidridei*, from Riversleigh's high FZ C JJ Site, occupies the highest position on the morphocline owing to its more derived character states.

In regard to *Ne. scottorrorum*, the high degree of morphological variation in the development of cusps, crests and cingula evident in *Ne. tirarensis* and *Ne. stirtoni* populations, suggests the single feature listed by Murray et al. (2000b) as distinguishing *Ne. scottorrorum* as a separate species of *Neohelos* does not merit taxonomic distinction. Murray et al. (2000b) tentatively retained *Ne. scottorrorum* as a separate species based on the presence of a distinct crest on the lingual face of the metaconule, a feature they viewed as morphologically intermediate between *Ne. solus* (*Neohelos* sp. A, Murray et al. 2000b) and *Ne. tirarensis*. The FT maxilla (QM F23157) was published as the holotype and only known specimen of *Nimbadon scottorrorum* (Hand et al. 1993). Black and Archer (1997b) suggested the specimen was more appropriately referred to *Neohelos*, and was most similar to FZ A *Neohelos* specimens from Riversleigh and forms intermediate between the small FZ A forms and characteristic *Ne. tirarensis* material from FZ B. All of the Riversleigh FZ A and FZ B material has subsequently been assigned to *Ne. tirarensis* (Murray et al. 2000b). Consequently, QM F23157 is here regarded as a chronomorph of *Ne. tirarensis*. In terms of premolar morphology and dimensions (Fig. 7B), it is most similar to QM F40163 from the Bone Reef LF (FZ A). On the basis of molar dimensions, however, it groups consistently with *Ne. tirarensis* specimens from Riversleigh's FZ B sites, and with specimens from the Kutjamarpu LF (Fig. 7D, F).

A left maxilla with P3–M3 (QM F30878) from COA Site, nominated by Murray et al. (2000b) as the reference speci-

men for *Neohelos* sp. A, is here designated as the holotype of *Neohelos solus*. Description of additional material from the type locality in the present analysis tentatively supports Murray et al.'s (2000b) hypothesis that the COA sample represents a single, distinct species of *Neohelos*. Coefficients of variation of dental dimensions (except for those of M4) generally fall within expected levels (4–10; Simpson et al. 1960) for a single mixed-sex population (Table 2). However, as noted by Murray et al. (2000b), in some aspects of morphology *Ne. solus* is indistinguishable from *Ne. tirarensis*. Specific distinctions are not obvious based on the morphology of most of the upper (M1 being an exception, see below) and lower cheekteeth. This is at least in part the result of the high degree of variation in premolar morphology characteristic of the genus, as well as the generalized, simple lophodont structure of the molars. Further, on the basis of premolar dimensions (Figs. 7A, B, 8A), *Ne. solus* is similar to small *Ne. tirarensis* specimens from FZ A sites (SB, UBO, D) and FZ B sites (MM, DT, FT) at Riversleigh. As noted by Murray et al. (2000b), consistent morphological differences between *Ne. solus* and *Ne. tirarensis* can only be found in the first upper molar. The most notable differences include the narrower, more arcuate M1 protoloph and the extension of the posterolingual cingulum along the lingual face of the metaloph in *Ne. solus* (Fig. 9). Analysis of M1 dimensions further indicates a distinction between the species (Figs. 7C, E, 8B–D), with *Ne. solus* M1s being proportionately narrower with respect to their length.

All M1s (n = 17) recovered from the COA deposit were confidently assigned to *Neohelos* sp. A by Murray et al. (2000b). Because of the absence of any undoubted *Ne. tirarensis* M1s in the sample, Murray et al. (2000b) assigned the entire COA sample to *Neohelos* sp. A. For the same reason, the additional material described in this study (which includes three M1s) is referred above to *Ne. solus* (*Neohelos* sp. A of Murray et al. 2000b).

A left P3–M1 (QM F56138) from the KCB LF is tentatively referred to *Ne. solus* rather than *Ne. tirarensis* because its M1 displays characteristic features of the latter, including convex paracone and metacone buccal margins, a weak postmetacrista and strong stylar cusp E, a discontinuous lingual cingulum, an arcuate protoloph with a deep cleft on its posterior face, and a posterolingual cingulum that ascends the lingual face of the metaloph.

If both *Ne. tirarensis* and *Ne. solus* are present at KCB, this is the first occurrence of more than one species of the genus in a single deposit. Whether these taxa were truly contemporaneous or whether their shared presence is the result of deposition over a considerable period of time is unknown. Keith's Chocky Block is a very unusual site in appearing to represent a vertical fissure or filling of a vertical cave neck (Creaser 1997). Not all of the material from this deposit is therefore necessarily contemporaneous. On the basis of faunal composition as a whole, Travouillon et al. (2006) hypothesized that KCB groups most closely with FZ C deposits such as Gag and Henk's Hollow sites. Gillespie (2007) also

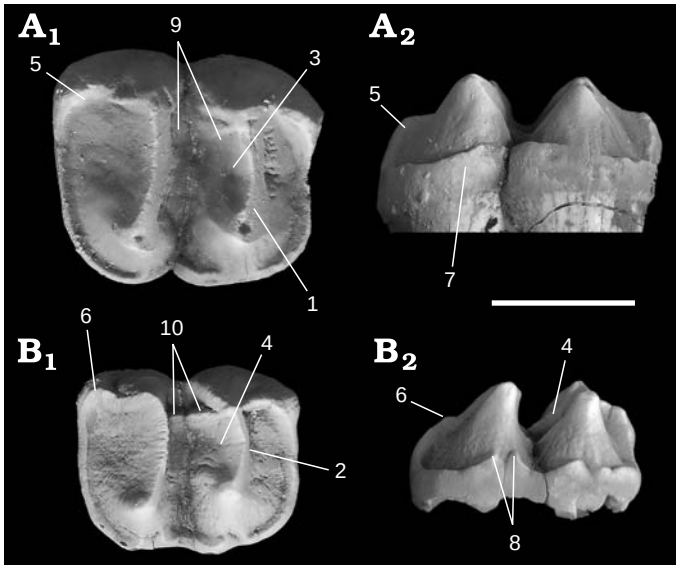

Fig. 9. Comparison of diprotodontid marsupials *Neohelos tirarensis* Stirton, 1967 (QMF 30438) (**A**) and *Neohelos solus* sp. nov. (QMF29739) (**B**) first upper molars (M1) in occlusal (A_1, B_1) and lingual (A_2, B_2) views. In addition to differences in size and relative width the following distinctions are evident: 1, elongate protoloph compared with; 2, short, arcuate protoloph; 3, shallow posterior face of protoloph compared with; 4, deep cleft on posterior face of protoloph; 5, broad, high stylar cusp E compared with; 6, weak, low stylar cusp E; 7, lingual cingulum low compared with; 8, lingual cingulum ascends lingual surface of metaconule; 9, weak postparacrista and weak/absent premetacrista compared with; 10, distinct postparacrista and premetacrista that meet in the interloph valley. Scale bar 10 mm.

suggested a FZ C age for KCB because it contains *Wakaleo oldfieldi*, which is also known from the HH, GS, and JJ LFs as well as the COA LF. The two *Neohelos* premolars from KCB do little to pin the position of this deposit on the *Neohelos* morphocline, because these teeth vary considerably in size and associated structures.

A fragmented maxilla with dP3 and P3–M2 from the JJ Site, nominated by Murray et al. (2000b) as the reference specimen for *Neohelos* sp. C, is herein designated the holotype of *Neohelos davidridei*. On the basis of premolar dimensions, *Ne. davidridei* is the largest diprotodontoid species, and consequently the largest marsupial species, currently known from Riversleigh's Oligo-Miocene deposits. Although similar overall to *Ne. stirtoni*, it is named a distinct species based on its possession of a number of derived character states including: higher crowned molars, an incipiently divided parametacone on P3, a large parastyle on P3, and loss of the anterior protoconid crest on p3. The incipiently divided parametacone is a prelude to the condition found in younger (i.e., Late Miocene), more derived zygomaturine diprotodontids such as *Kolopsis* species, in which the parametacone is completely separated into two cusps, the paracone and metacone. As noted by Murray et al. (2000b), *Ne. davidridei* has a P3 morphology structurally transitional between that of *Ne. stirtoni* and *Kolopsis yperus* from the Late Miocene Ongeva LF of the Northern Territory. The type deposit for *Ne. davidridei*, JJ Site, is positioned at the strati-

http://dx.doi.org/10.4202/app.2012.0001

graphically highest (201 m) level of the northern section of Riversleigh's Gag Plateau sequence (Creaser 1997). The large size and derived nature of the dentition of *Ne. davidridei* are in agreement with its stratigraphic position and support a Middle Miocene, high FZ C age for the deposit.

Additional material of *Ne. stirtoni* is described from the Gag, HH, and GS deposits at Riversleigh. Reanalysis of specimens QM F40172 (AR13791) and QM F40173 from SB Site, originally assigned to *Ne. stirtoni* by Murray et al. (2000b), suggests they are more appropriately referred to *Ngapakaldia bonythoni* and *Ne. tirarensis*, respectively (Black 2010). Consequently, *Ne. stirtoni* is restricted to Riversleigh's FZ C deposits, which is in agreement with its relatively derived phylogenetic position within the genus. By comparison with *Ne. tirarensis* and *Ne. solus*, *Ne. stirtoni* is a relatively rare component at Riversleigh, represented by only seven specimens from three deposits. This is in direct contrast with the high abundance of *Ne. stirtoni* material found at the type locality at Bullock Creek, Northern Territory. *Neohelos stirtoni* is contemporaneous with *Ni. lavarackorum* at Bullock Creek and in two FZ C deposits at Riversleigh: Gag Site and HH (Black and Hand 2010). Interestingly, where *Ne. stirtoni* is abundant, *Ni. lavarackorum* is rare, and vice versa. For example, at Bullock Creek, hundreds of specimens of *Ne. stirtoni* have been recovered including complete skulls and postcranial elements (Murray et al. 2000a, b), with at least 27 individuals represented (based on upper right premolar abundance). In stark contrast, *Ni. lavarackorum* is represented at Bullock Creek by a single maxilla. These extremes of abundance are probably a reflection of the different habitats occupied by the two species, with some minimal overlap in home range.

Table 3. *Neohelos tirarensis* univariate statistics. Sites with more than one specimen were scored from a single side only. Abbreviations: AW, anterior width; CV, coefficient of variation; L, length; Max, maximum value; Min, minimum value; N, sample size; PW, posterior width; SD, standard deviation; SE, standard error; W, width.

	N	Min	Max	Mean	SE	SD	Median	CV
P3L	14	13.8	16.8	15.6	0.2	1.0	15.7	6.2
P3W	15	12.3	15.1	13.8	0.2	0.9	13.6	6.6
M1L	9	14.8	17.4	16.4	0.2	0.9	16.4	5.3
M1AW	7	14.2	15.0	14.7	0.1	0.3	14.7	1.9
M1PW	8	14.1	15.8	14.8	0.1	0.6	14.8	3.9
M2L	9	16.7	18.3	17.5	0.1	0.6	17.3	3.3
M2AW	8	14.9	16.9	16.0	0.1	0.7	16.3	4.3
M2PW	8	13.3	16.2	15.2	0.2	0.9	15.3	5.9
M3L	7	17.1	19.6	18.4	0.2	1.0	18.5	5.5
M3AW	5	15.2	17.8	16.7	0.2	0.9	16.8	5.6
M3PW	6	14.1	15.6	14.9	0.1	0.6	14.8	3.9
M4L	5	17.0	19.4	18.3	0.2	0.9	18.1	5.2
M4AW	4	15.0	16.5	15.8	0.1	0.6	15.9	3.9
M4PW	4	12.1	13.5	12.9	0.1	0.6	12.9	4.5
p3L	6	12.0	13.4	12.7	0.2	0.5	12.8	4.1
p3W	6	8.2	10.0	8.7	0.2	0.7	8.5	7.5
m1L	7	15.3	17.4	16.5	0.2	0.8	16.5	4.8
m1AW	7	10.3	12.6	11.1	0.2	0.8	10.8	7.2
m1PW	7	11.2	13.3	12.0	0.2	0.7	11.9	6.0
m2L	3	16.0	18.7	17.7	0.4	1.5	18.5	8.5
m2AW	3	12.3	15.5	13.9	0.5	1.6	13.9	11.5
m2PW	3	12.7	14.5	13.9	0.3	1.0	14.4	7.3
m3L	5	17.0	19.7	18.8	0.3	1.1	19.2	5.8
m3AW	5	13.0	15.4	14.3	0.3	0.9	14.2	6.4
m3PW	5	12.2	14.4	13.6	0.2	0.9	13.8	6.3
m4L	2	16.2	18.2	17.2	0.4	1.4	17.2	8.2
m4AW	2	12.1	14.1	13.1	0.4	1.4	13.1	10.8
m4PW	2	10.5	13.9	12.2	0.7	2.4	12.2	19.7

Biostratigraphy

The most complete, and consequently biochronologically most useful, phyletic succession of any Australian marsupial group has been recorded for the zygomaturine genus *Neohelos* (Murray et al. 2000b). All four species currently recognized are found at Riversleigh. The type species, *Ne. tirarensis,* was originally described from the Kutjamarpu LF from the Tirari Desert in South Australia, but has since been recognized in FZs A–C at Riversleigh (Murray et al. 2000b; this paper) and also from the Kangaroo Well LF in the Northern Territory (Megirian et al. 2004). In terms of morphology, *Ne. tirarensis* specimens from the type locality are most similar to those from FZ B and FZ C sites at Riversleigh (e.g., WW and KCB, respectively). However, if we consider tooth dimensions, the referred P3 (AMF87625) from the type locality is intermediate in size between material from FZ A and FZs B–C (Fig. 7B), while on the basis of M1 dimensions (Fig. 7D, F) material from Leaf Locality variably groups with *Ne. tirarensis* from FZs B (e.g., CS) and C (e.g., KCB) and *Ne. stirtoni* material from Bullock Creek.

Woodburne et al. (1993) suggested a Late Oligocene age for the Wipajiri Formation, the source for the Kutjamarpu LF. Archer et al. (1994, 1995) disagreed, suggesting instead an Early Miocene age for the deposit based on biocorrelation and the relative stage-of-evolution of its mammalian fauna. The Etadunna Formation, into which the Wipajiri Formation has cut, however, has been reliably dated as Late Oligocene (24–26 MY BP) on the basis of magnetostratigraphic data, foraminiferal stratigraphy and radioisotopic dates on illite (Woodburne et al. 1993). Most recently, Megirian et al. (2010) suggest a maximum age of 23.4 MY BP for the Wipajri Formation, with an age range of 23.4 MY BP to 17.6 MY BP.

In addition to *Ne. tirarensis*, eight other species are shared between the Kutjamarpu LF and Riversleigh's Oligo-Miocene assemblages. These include: *Emuarius gidju* (FZs A, B, C; Archer et al. 2006); the wombat *Rhizophascolonus crowcrofti* (FZs A, B, C; Archer et al. 2006); the koala *Litokoala kutjamarpensis* (FZ C; Black and Archer 1997a; Louys et al. 2007; Black et al. 2013); the potoroid *Wakiewakie lawsoni* (FZ B; Godthelp et al. 1989); the ektopodontid *Ektopodon serratus* (FZ B; Archer et al. 2006); the ringtail possums (Archer et al.

Table 4. Univariate statistics for *Neohelos stirtoni* from Blast Site, Bullock Creek, Northern Territory. Generated using data from tables 2–3 in Murray et al. (2000b). Right upper dentition and left lower dentition used only. Abbreviations: AW, anterior width; CV, coefficient of variation; L, length; Max, maximum value; Min, minimum value; N, sample size; PW, posterior width; SD, standard deviation; SE, standard error; W, width.

	N	Min	Max	Mean	SE	SD	Median	CV
P3L	21	16.0	20.2	18.4	0.2	1.1	18.3	6.2
P3W	19	15.0	17.6	16.0	0.1	0.7	15.8	4.5
M1L	20	17.2	21.7	19.6	0.2	1.0	19.6	5.0
M1AW	18	16.1	19.1	17.7	0.2	1.0	17.9	5.4
M1PW	17	16.4	20.2	18.2	0.2	0.9	17.9	5.2
M2L	20	19.6	22.9	21.6	0.2	0.8	21.7	3.7
M2AW	16	18.0	21.3	20.0	0.2	0.9	20.3	4.5
M2PW	18	18.1	21.4	19.4	0.2	0.9	19.2	4.8
tM3L	12	21.0	24.2	23.0	0.2	1.1	23.4	4.6
M3AW	12	19.3	22.4	21.0	0.2	1.0	21.1	4.6
M3PW	11	17.9	21.0	19.1	0.2	1.1	18.8	5.8
M4L	10	21.8	25.0	23.2	0.2	1.2	23.2	5.1
M4AW	9	18.2	22.0	19.9	0.2	1.2	20.0	5.9
M4PW	7	14.4	16.9	15.7	0.2	1.0	15.6	6.2
p3L	11	11.5	16.3	14.4	0.3	1.2	14.6	8.2
p3W	9	9.7	11.9	10.8	0.2	0.8	10.7	7.2
m1L	15	17.3	22.7	19.6	0.3	1.4	19.7	7.4
m1AW	13	12.4	16.7	13.8	0.2	1.1	13.7	7.9
m1PW	14	13.2	18.7	15.3	0.3	1.4	15.6	9.0
m2L	14	19.1	23.9	21.8	0.3	1.4	22.0	6.6
m2AW	11	15.6	18.3	17.3	0.2	0.9	17.3	5.0
m2PW	14	15.0	19.5	17.0	0.3	1.4	17.2	8.2
m3L	16	22.7	25.9	24.1	0.2	0.9	24.2	3.7
m3AW	15	17.0	21.4	18.6	0.2	1.1	18.5	6.1
m3PW	14	16.1	19.7	17.7	0.2	1.0	17.6	5.7
m4L	11	20.0	25.2	23.4	0.4	1.7	23.5	7.4
m4AW	9	17.2	18.9	18.1	0.1	0.6	18.3	3.3
m4PW	8	15.9	18.3	17.0	0.2	0.9	16.9	5.4

2006; Roberts et al. 2008, 2009): *Paljara tirarensae* (FZ B), *Marlu kutjamarpensis* (FZ C), *Marlu ampelos* (FZ C), and *Marlu syke* (FZs B–C); and the marsupial lion *Wakaleo oldfieldi* (FZ C; Gillespie 2007). Of these, seven taxa are restricted in their distribution to a single FZ at Riversleigh, but that FZ is not the same for each taxon, these being either FZ B or C. Travouillon et al. (2006) performed a series of multivariate analyses of presence/absence data for species from a range of Riversleigh deposits and the Kutjamarpu LF, but were unable to further refine the biostratigraphic position of the latter. On the basis of current shared taxa, the Kutjamarpu LF apparently lies somewhere between Early Miocene (FZ B) and Middle Miocene (FZ C) time.

Megirian et al. (2004) noted the presence of *Ne. tirarensis* in the Kangaroo Well LF from the Ulta Limestone in the Northern Territory. Although the specimen is too fragmentary to assist with biocorrelation of the deposit, the presence of a new species of ektopodontid, *Ektopodon ulta*, which is more derived than *E. stirtoni* from the Ngama LF (Etadunna FZ D), yet plesiomorphic relative to *E. litolophus* from the Kutjamarpu LF, suggests a Late Oligocene to Early Miocene age for the Kangaroo Well LF. Megirian et al. (2004) did, however, note that this age estimation is based on the assumption that the paleomagnetic dates given for the Etadunna and Wipajiri formations are correct. Megirian et al. (2004) also suggested, on the basis of their analysis of faunal similarity (mainly generic level diversity), that the Kangaroo Well LF groups with the "Carl Creek Limestone vertebrate assemblage" (FZs A–C) [sic!]. Diagnostic *Ne. tirarensis* material, such as P3 or M1, from the Kangaroo Well LF will assist with refining the relative age of this deposit compared with the Early to Middle Miocene Kutjamarpu LF and Riversleigh's Oligocene and Miocene fossil assemblages.

The presence of small chronomorphs of *Ne. tirarensis* in Riversleigh's FZ A deposits, forms more plesiomorphic than *Ne. tirarensis* from the Kutjamarpu LF, corroborate the overall understanding (e.g., Creaser 1997) that some of Riversleigh's stratigraphic units predate the Wipajiri Formation (Murray et al. 2000b). Fragmentary remains of *Neohelos* have been recovered from FZs D–E of the Etadunna Formation, but these have not yet been diagnosed to species level (Woodburne et al. 1993). Myers and Archer (1997) have previously demonstrated a species correlation between Riversleigh's WH Site (FZ A) and Mammalon Hill (Ngama LF, Faunal Zone D of the Etadunna Formation), a deposit dated magnetostratigraphically to 24.1 MY BP (Megirian et al. 2010). More recently, *Ne. tirarensis* has also been discovered at the White Hunter Site at Riversleigh. This material is similar in size to material from the SB LF and Site D (= the Riversleigh LF), suggesting a Late Oligocene age for these deposits.

The shared presence of *Propalorchestes novaculacephalus*, *Nimbadon lavarackorum*, and *Neohelos stirtoni* in Riversleigh's low to mid FZ C assemblages (Black 1997, 2006; Murray et al. 2000b; Black and Hand 2010) confirms previous hypotheses (Archer et al. 1989, 1994, 1995) that they are of a similar age to the Middle Miocene Bullock Creek LF. The presence of *Ne. davidridei*, the largest and most derived species of *Neohelos*, in the JJ assemblage at Riversleigh suggests that this high FZ C deposit is younger than the Bullock Creek LF, but predates the Late Miocene deposits of the Waite Formation. *Neohelos davidridei* exhibits an upper third premolar morphology that anticipates the condition found in the more derived zygomaturines *Kolopsis* spp., which first appear in the Late Miocene Alcoota and Ongeva LFs of the Waite Formation, Northern Territory.

Analysis of diprotodontoid faunas has allowed an assessment of the relative age of some Riversleigh deposits of previously uncertain age. Based on the stage-of-evolution of *Ne. tirarensis* specimens represented, the following sites are interpreted to be FZ B deposits: Dunsinane, FT, CR, and DT. The large, derived nature of *Ne. tirarensis* specimens from BC 2 Site (Fig. 7B) supports Creaser's (1997) FZ C allocation for this deposit. In the COA LF, the presence of *Ni. lavarackorum* is indicative of an FZ C age (Black and Hand

http://dx.doi.org/10.4202/app.2012.0001

2010). The presence of *Ne. solus* and *Wakaleo oldfieldi* (Gillespie 2007) in both the COA and KCB LFs suggests these deposits are of equivalent age, and hence the latter is also interpreted to be an FZ C deposit.

Conclusions

With our description of two new species, the zygomaturine genus *Neohelos* now comprises: *Ne. tirarensis*, *Ne. stirtoni*, *Ne. solus* sp. nov., and *Ne. davidridei* sp. nov. All four species occur in Oligo-Miocene sediments at Riversleigh, with the latter two species being unique to this locality. *Neohelos solus* (= *Neohelos* sp. A of Murray et al. 2000b) is described from the COA and KCB LFs and, on the basis of its more elongate, rectangular upper molars, is regarded to be the most plesiomorphic member of the genus. *Neohelos davidridei* (= *Neohelos* sp. C of Murray et al. 2000b) is unique to the high FZ C JJ LF and is the most derived member of the genus, displaying a number on features of P3 (including an incipiently divided parametacone) that are structurally antecedent to species of *Kolopsis*. A chronological morphocline (noted by Murray et al. 2000b) evidenced by a gradual change in morphology accompanied by an increase in size, is recorded from *Ne. tirarensis*, through *Ne. stirtoni*, to *Ne. davidridei*. This morphocline is most strongly reflected in molar size (rather than the more variable premolar) and is generally consistent with the biostratigraphic distribution of *Neohelos* species throughout the Riversleigh FZs as proposed by Archer et al. (1989, 1994, 1997).

Five diprotodontoid species from Riversleigh allow direct biocorrelation with other Australian Tertiary mammal faunas. Comparison of *Ne. tirarensis* material from Riversleigh's FZ A–C deposits with that from the type locality, Leaf Locality, Kutjamarpu LF, Wipajiri Formation, South Australia cannot refine the relative ages of these deposits. However, on the basis of other shared species, the Kutjamarpu LF sits somewhere between Riversleigh's Early Miocene (FZ B) and Middle Miocene (FZ C) faunas, refuting a Late Oligocene age for the deposit (Woodburne et al. 1993). The presence of plesiomorphic chronomorphs of *Ne. tirarensis* in some FZ A deposits suggests that Riversleigh's basal sediments predate the South Australian Wipajiri Formation. *Neohelos tirarensis* is now known from the WH LF, which has previously been correlated with the Ngama LF (Faunal Zone D) of the Etadunna Formation a deposit dated magnetostratigraphically to 24.7–25 MY BP (Woodburne et al. 1993). The shared presence of *Ng. bonythoni* in several FZ A local faunas at Riversleigh and the Ngapakaldi LF (Faunal Zone C) of the Etadunna Formation, lends further support to a Late Oligocene age for these Riversleigh deposits (Black 2010).

A strong faunal correlation exists between Riversleigh's low to mid Faunal Zone C deposits and the Middle Miocene Bullock Creek LF of the Northern Territory. They share three diprotodontoid species: *Propalorchestes novaculacephalus*, *Ne. stirtoni*, and *Ni. lavarackorum* (Black 1997, 2006; Murray et al. 2000b; Black and Hand 2010). In the high FZ C Jaw Junction LF, the presence of *Ne. davidridei*, a form more derived than *Ne. stirtoni*, suggests that this deposit is younger than the Bullock Creek LF.

Acknowledgements

Vital assistance in the field has come from many hundreds of volunteers as well as staff and postgraduate students of the University of New South Wales, Sydney, Australia. Skilled preparation of much of the material described in this paper has been carried out by Anna Gillespie (University of New South Wales). We thank the late Dirk Megirian (Northern Territory Museum, Alice Springs, Australia) for providing access to comparative material, and Peter Murray (Northern Territory Museum, Alice Springs, Australia) for his invaluable insight and discussions regarding the *Neohelos* sample. We also thank the reviewers Julien Louys (Australian National University, Canberra, Australia) and Gilbert Price (University of Queensland, Brisbane, Australia) for their thoughtful comments. Support for Riversleigh research has been provided by the Australian Research Council (DE130100467, DP043262, DP1094569, LP0453664, LP0989969, LP100200486), Xstrata Community Partnership Program North Queensland, Queensland Parks and Wildlife Service, Environment Australia, the Queensland and Australian Museums, University of New South Wales, Phil Creaser and the CREATE Fund at UNSW, Outback at Isa, Mount Isa City Council and the Waanyi people of northwestern Queensland.

References

Aplin, K.P. and Archer, M. 1987. Recent advances in marsupial systematics with a new syncretic classification. *In*: M. Archer (ed.), *Possums and Opossums: Studies in Evolution*, xv–lxxii. Surrey Beatty and Sons Pty Ltd., Chipping Norton, New South Wales.

Archer, M. 1984. The Australian marsupial radiation. *In*: M. Archer and G. Clayton (eds.), *Vertebrate Zoogeography and Evolution in Australasia*, 633–808. Hesperian Press, Perth.

Archer, M., Hand, S.J., and Godthelp, H. 1994. *Riversleigh*. 264 pp. Reed Books Pty Ltd, Sydney.

Archer, M., Hand, S.J., and Godthelp, H.J. 1995. Tertiary environmental and biotic change in Australia. *In*: E. Vrba, G.H. Denton, T.C. Partridge, and L.H. Burckle (eds.), *Palaeoclimate and Evolution, with Emphasis on Human Origins*, 77–90. Yale University Press, New Haven.

Archer, M., Godthelp, H., Hand, S., and Megirian, D. 1989. Fossil mammals of Riversleigh, northwestern Queensland: preliminary overview of biostratigraphy, correlation and environmental change. *Australian Zoologist* 25 (2): 29–65.

Archer, M., Hand, S.J., Godthelp, H., and Creaser, P. 1997. Correlation of the Cainozoic sediments of the Riversleigh World Heritage Fossil Property, Queensland, Australia. *In*: J.-P. Aguilar, S. Legendre, and J. Michaux (eds.), *Actes du Congres BiocroM'97*, 131–152. Memoirs et Traveaux Ecole Pratique des Hautes Etudes, Institut de Montpellier, Montpellier.

Archer, M., Arena, D.A., Bassarova, M., Beck, R.M.D., Black, K., Boles, W.E., Brewer, P., Cooke, B.N., Crosby, K., Gillespie, A., Godthelp, H., Hand, S.J., Kear, B.P., Louys, J., Morrell, A., Muirhead, J., Roberts, K.K., Scanlon, J.D., Travouillon, K.J., and Wroe, S. 2006. Current status of species-level representation in faunas from selected fossil localities in the Riversleigh World Heritage Area, northwestern Queensland. *Alcheringa* 30 (2 Supplement 1): 1–17.

Black, K. 1997. Diversity and biostratigraphy of the Diprotodontoidea of

Riversleigh, northwestern Queensland. *Memoirs of the Queensland Museum* 41: 187–192.

Black, K. 2006. Description of new material for *Propalorchestes novaculacephalus* (Marsupialia: Palorchestidae) from the mid Miocene of Riversleigh, northwestern Queensland. *Alcheringa: An Australasian Journal of Palaeontology* 30 (2): 351–361.

Black, K.H. 2010. *Ngapakaldia bonythoni* (Marsupialia, Diprotodontidae): new material from Riversleigh, northwestern Queensland, and a reassessment of the genus *Bematherium*. *Alcheringa* 34: 471–492.

Black, K. and Archer, M. 1997a. *Nimiokoala* gen. nov. (Marsupialia, Phascolarctidae) from Riversleigh, northwestern Queensland, with a revision of *Litokoala*. *Memoirs of the Queensland Museum* 41: 209–228.

Black, K. and Archer, M. 1997b. *Silvabestius*, a new genus and two new species of primitive zygomaturines (Marsupialia, Diprotodontidae) from Riversleigh, northwestern Queensland. *Memoirs of the Queensland Museum* 41: 181–208.

Black, K. and Mackness, B. 1999. Diversity and relationships of diprotodontoid marsupials. *Australian Mammalogy* 21: 20–21, 34–45.

Black, K.H. and Hand, S.J. 2010. First crania and assessment of species boundaries in *Nimbadon* (Marsupialia: Diprotodontidae) from the middle Miocene of Australia. *American Museum Novitates* 3678: 1–60.

Black, K.H., Archer, M., Hand, S.J., and Godthelp, H. 2012a. The rise of Australian marsupials: a synopsis of biostratigraphic, phylogenetic, palaeoecological and palaeobiogeographic understanding. *In*: J.A. Talent (ed.), *Earth and Life: Global Biodiversity, Extinction Intervals and Biogeographic Perturbations through Time*, 983–1078. Springer Verlag, Dordrecht.

Black, K.H., Camens, A.B., Archer, M., and Hand, S.J., 2012b. Herds overhead: N*imbadon lavarackorum* (Diprotodontidae), heavyweight marsupial herbivores in the Miocene forests of Australia. *PLoS ONE* 7, e48213.

Black, K.H., Louys, J., and Price, G.J. 2013. Understanding morphological variation in the extant koala as a framework for identification of species boundaries in extinct koalas (Phascolarctidae; Marsupialia). *Journal of Systematic Palaeontology*.

Creaser, P. 1997. Oligocene–Miocene sediments of Riversleigh: the potential significance of topography. *Memoirs of the Queensland Museum* 41: 303–314.

Flower, W. 1867. On the development and succession of teeth in the Marsupialia. *Philosophical Transactions of the Royal Society London* 157: 631–641.

Gill, T. 1872. Arrangement of the families of mammals with analytical tables. *Smithsonian Miscellaneous Collections* 11 (1): 98.

Gillespie, A.K. 2007. *Diversity and Systematics of Marsupial Lions from The Riversleigh World Heritage Area and the Evolution of the Thylacoleonidae*. xii + 394 pp. Unpublished Ph.D. thesis, The University of New South Wales, Sydney.

Godthelp, H., Archer, M., Hand, S.J., and Plane, M.D. 1989. New potoroine from Tertiary Kangaroo Well Local Fauna, Northern Territory and description of upper dentition of potoroine *Wakiewakie lawsoni* from Upper Site Local Fauna, Riversleigh. *In*: *5th Conference on Australian Vertebrate Evolution, Palaeontology and Systematics, Abstracts*, 6. University of New South Wales, Sydney.

Hammer, Ø., Harper, D., and Ryan, P. 2001. PAST: Paleontological Statistics Software Package for Education and Data Analysis. *Palaeontologia Electronic*a 4: 1–9.

Hand, S., Archer, M., Rich, T., and Pledge, N. 1993. *Nimbadon*, a new genus and three species of Tertiary zygomaturines (Marsupialia, Diprotodontidae) from northern Australia, with a reassessment of *Neohelos*. *Memoirs of the Queensland Museum* 33: 193–210.

Illiger, C. 1811. *Prodromus systematis mammalium et avium additis terminis zoographicis utriudque classis*. xviii + 301 pp. C. Salfeld, Berlin.

Louys, J., Black, K., Archer, M., Hand, S.J., and Godthelp, H. 2007. Descriptions of koala fossils from the Miocene of Riversleigh, northwestern Queensland and implications for *Litokoala* (Marsupialia, Phascolarctidae). *Alcheringa* 31: 99–110.

Luckett, W.P. 1993. An ontogenetic assessment of dental homologies in therian mammals. *In*: F.S. Szalay, M.J. Novacek, and M.C. McKenna (eds.), *Mammal Phylogeny: Mesozoic Differentiation, Multituberculates, Monotremes, Early Therians and Marsupials*, 182–204. Springer-Verlag, New York.

Megirian, D., Murray, P., Schwartz, L., and Von der Borch, C. 2004. Late Oligocene Kangaroo Well Local Fauna from the Ulta Limestone (new name), and climate of the Miocene oscillation across central Australia. *Australian Journal of Earth Sciences* 51: 701–741.

Megirian, D., Prideaux, G.J., Murray, P.F., and Smit, N. 2010. An Australian land mammal age biochronological scheme. *Paleobiology* 36: 658–671.

Murray, P., Megirian, D., Rich, T., Plane, M., and Vickers-Rich, P. 2000a. *Neohelos stirtoni*, a new species of Zygomaturinae (Diprotodontidae: Marsupialia) from the mid-Tertiary of northern Australia. *Memoirs of the Queen Victoria Museum* 105: 1–47.

Murray, P., Megirian, D., Rich, T., Plane, M., Black, K., Archer, M., Hand, S., and Vickers-Rich, P. 2000b. Morphology, systematics, and evolution of the marsupial genus *Neohelos* Stirton (Diprotodontidae, Zygomaturinae). *Museums and Art Galleries of the Northern Territory Research Report* 6: 1–141.

Myers, T. and Archer, M. 1997. *Kuterintja ngama* (Marsupialia, Ilariidae): a revised systematic analysis based on material from the late Oligocene of Riversleigh, northwestern Queensland. *Memoirs of the Queensland Museum* 41: 379–392.

Owen, R. 1866. *On the Anatomy of Vertebrates. Vol. 2, Birds and Mammals*. 592 pp. Longmans Green, London.

Price, G.J. 2008. Taxonomy and palaeobiology of the largest-ever marsupial, *Diprotodon* Owen, 1838 (Diprotodontidae, Marsupialia). *Zoological Journal of the Linnean Society* 153: 369–397.

Price, G.J. and Piper, K.J. 2009. Gigantism of the Australian *Diprotodon* Owen 1838 (Marsupialia, Diprotodontoidea) through the Pleistocene. *Journal of Quaternary Science* 24: 1029–1038.

Price, G.J. and Sobbe, I.H. 2010. Morphological variation within an individual Pleistocene *Diprotodon optatum* Owen, 1838 (Diprotodontinae; Marsupialia): implications for taxonomy within diprotodontoids. *Alcheringa: An Australasian Journal of Palaeontology* 35: 21–29.

Rich, T.H., Archer, M., and Tedford, R.H. 1978. *Raemeotherium yatkolai*, gen. et sp. nov., a primitive diprotodontid from the medial Miocene of South Australia. *Memoirs of the National Museum of Victoria* 39: 85–91.

Roberts, K.K., Bassarova, M., and Archer, M. 2008. Oligo-Miocene ringtail possums of the genus *Paljara* (Pseudocheiridae: Marsupialia) from Queensland, Australia. *Geobios* 41: 833–844.

Roberts, K.K., Archer, M., Hand, S.J., and Godthelp, H. 2009. New Australian Oligocene to Miocene ringtail possums (Pseudocheiridae) and revision of the genus *Marlu*. *Palaeontology* 52: 441–456.

Simpson, G., Roe, A., and Lewontin, R. 1960. *Quantitative Zoology*. 440 pp. Harcourt Brace, New York.

Stirton, R. 1967. A diprotodontid from the Miocene Kutjamarpu Fauna, South Australia. *Bureau of Mineral Resources, Geology and Geophysics Bulletin* 85: 45–51.

Stirton, R., Woodburne, M., and Plane, M. 1967. A phylogeny of the Tertiary Diprotodontidae and its significance in correlation. *In*: R. Stirton, M. Woodburne, and M. Plane (eds.), *Bureau of Mineral Resources, Geology and Geophysics, Australia, Bulletin* 85: 45–51.

Tedford, R.H. and Woodburne, M.O. 1987. The Ilariidae, a new family of vombatiform marsupials from Miocene strata of South Australia and an evaluation of the homology of molar cusps in the Diprotodontia. *In*: M. Archer (ed.), *Possums and Opossums: Studies in Evolution*, 401–418. Surrey Beatty and Sons Pty Ltd, Chipping Norton, New South Wales.

Travouillon, K.J., Archer, M., Hand, S.J., and Godthelp, H. 2006. Multivariate analyses of Cenozoic mammalian faunas from Riversleigh, northwestern Queensland. *Alcheringa* 30 (2 Supplement 1): 323–349.

Woodburne, M.O., MacFadden, B.J., Case, J.A., Springer, M.S., Pledge, N.S., Power, J.D., Woodburne, J.M., and Springer, K.B. 1993. Land mammal biostratigraphy and magnetostratigraphy of the Etadunna Formation (late Oligocene) of South Australia. *Jounal of Vertebrate Paleontology* 13: 483–515.

http://dx.doi.org/10.4202/app.2012.0001

Appendix 1

List of AR specimens used in Murray et al. (2000a) and their designated QM F numbers.

AR	QM F	AR	QM F
1685	41043	11858	40145
1686	41044	12120	40138
3850	40168	13360	40139
3878	40165	13795	40130
4294	40166	13969	40173
5621	40174	13994	40131
5797	40175	14393	40146
5896	40167	15119	40150
5989	40176	15239	40156
6343	40177	15751	40151
6685	40170	16492	40151
7726	40169	16596	40164
7851	40178	16656	40152
7857	40179	16787	40157
7858	40182	16810	40158
7859	40180	16955	40159
7860	40181	16957	40160
9925	40147	17291	40153
9947	40133	17443	40140
10362	40134	17453	40161
10458	40155	17454	40162
10641	40135	17469	40163
10668	40148	17470	40132
10669	40149	24239	40141
10706	40136	24240	40154
10726	40137		

Appendix 2

Table A. *Neohelos* spp. upper dental measurements (in mm). Abbreviations: AW, anterior width; L, length; PW, posterior width; W, width. Leaf refers to material from the Leaf Locality, Kutjamarpu Local Fauna. Specimens asterisked are taken from Murray et al. (2000a).

Specimen	Site	P3		M1			M2			M3			M4		
		L	W	L	AW	PW	L	AW	PW	L	AW	PW	L	AW	PW
Neohelos tirarensis															
QM F40132	BR	14.3	13.4												
QM F24137	BR			17.9	14.5	14.8	17.9	15.9	15.0	18.7	16.0	14.3			
QM F40133*	CS	16.6	14.7												
QM F40134*	CS						18.3	16.9	16.2						
QM F40136*	CS	16.5	12.5												
QM F40137*	CS	17.0	14.1												
QM F40138*	CS									18.4	17.8	15.6	19.4	16.5	13.5
QM F40140*	CS			16.9	15.0	15.1	17.0	15.9	15.0						
QM F40145*	JJS	16.8	12.9												
QML935	Dun	16.3	14.3	18.1			18.6	17.9	17.1	18.9	18.3		18.6	18.3	
QM F56239*	SB								16.5	20.1	19.5	17.2	20.5	19.1	14.5
QM F40130*	SB		12.3	14.8											
QM F40131*	SB	14.5	13.0												
QM F40147*	MM						18.1	16.4	15.5						

Specimen	Site	P3		M1			M2			M3			M4		
		L	W	L	AW	PW	L	AW	PW	L	AW	PW	L	AW	PW
QM F40150*	MM	16.8	13.6												
QM F40151*	MM	15.6	14.8	16.4	14.7	15.4	17.2	16.4	15.4	19.6	16.8	15.5	19.0	15.9	13.0
QM F40153*	NG									19.5	16.8	14.6			
QM F56135	WW	16.3	15.0	17.4	14.8	14.6	18.0	16.4	15.2				17.9	15.8	12.8
QM F56237	DT	14.8	13.4												
QM F56236	CR	16.6	13.6												
CPC22558*	Site D	15.4	13.7				19.2	17.1	15.7						
QM F13088L*	Inab	16.4	14.3	17.2	14.6	14.9	17.3	16.2	16.0	17.1	16.7	15.0			
QM F13088R*	Inab			17.2	14.5	14.8	17.0	16.0	15.8						
QM F40124*	BO	15.1	14.2												
QM F40129*	UBO						16.5	15.1	14.9	16.9	15.5	14.0	17.2	15.6	13.5
QM F40129*	UBO	13.8	12.4	15.4		14.4	16.7	15.1	14.7	17.1	15.2	14.1	17.0	15.0	12.1
QM F56238	KCB	16.1	14.2												
QM F56137	KCB	17.5	14.8	17.3	15.7	16.2									
QM F36321	BC2	16.9	15.5												
QM F23157*	FT	14.3	13.4	17.1	15.0	15.8	17.9			18.5			18.1		
AR456*	Leaf			18.7	16.6	16.9									
SAM/UC465*	Leaf			18.8	16.6	16.9									
UCMP69977	Leaf			17.0	15.5	15.6									
UCMP69978	Leaf						19.0	17.1	16.6						
AMF87625*	Leaf	15.8	13.9												
AMF87626*	Leaf						18.8	17.2	15.8						
Neohelos solus															
QM F30878*	COA	14.4	12.9	15.4	12.7	13.5	16.7	14.3	15.6	17.2	15.5	13.6			
QM F40160*	COA			16.9	13.8	14.2									
QM F40161*	COA						17.4	15.3	14.5						
QM F40162*	COA			16.9	13.7	13.3									
QM F40163*	COA												19.1	16.9	13.4
QM F12433*	COA												17.6	15.0	12.0
QM F12434*	COA			17.1	14.0	14.0									
QM F20488*	COA						17.6	15.8	14.5						
QM F20584*	COA	14.8	13.4												
QM F20585*	COA						17.0	15.3	14.9						
QM F20831*	COA									18.3	16.3	14.2			
QM F20852*	COA			16.8	13.1	13.1									
QM F22765*	COA						17.0	14.5	14.0	17.5	15.0	13.5			
QM F22765*	COA						17.1	14.7	14.3	17.8	15.2	13.8			
QM F22767*	COA									17.4	15.9	13.7			
QM F22771*	COA												17.5	14.6	11.5
QM F22773*	COA	14.1	12.6												
QM F23195*	COA			17.3	14.1	14.1									
QM F23197*	COA			16.7	14.0	13.9									
QM F23274*	COA	14.6	12.6												
QM F23407*	COA			16.0	13.8	14.1									
QM F23408*	COA									18.1	16.1	14.2			
QM F23472*	COA			16.0	13.2	13.3									
QM F24270*	COA			16.1	14.0	13.9	17.2	15.7	14.0	17.2	15.5	13.6			
QM F24299*	COA						17.5	15.0	14.6						
QM F24731*	COA			15.5	12.9	12.4									
QM F24741*	COA									18.3		14.4			
QM F29739*	COA			17.7	15.0	14.7									
QM F29740*	COA			16.0	13.1	13.7									
QM F30305*	COA			16.7	13.9	14.0	16.9	15.5	14.3	18.1	15.3	13.7			
QM F30556*	COA			15.7	13.5	13.8									
QM F30558*	COA			16.9	14.3	14.2									
QM F30734*	COA	15.5	13.8												
QM F31340	COA									17.9	16.4	13.7			
QM F31356	COA			15.9	13.1	13.2									

http://dx.doi.org/10.4202/app.2012.0001

Specimen	Site	P3		M1			M2			M3			M4		
		L	W	L	AW	PW	L	AW	PW	L	AW	PW	L	AW	PW
QM F50481	COA	14.2	12.0												
QM F50486	COA			16.5	13.1	13.5									
QM F50488	COA	14.6	13.5												
QM F50492	COA						18.7		14.0						
QM F50493	COA									17.4	15.2	13.1			
QM F50494	COA												16.2	13.9	11.4
QM F56232	COA	14.0	12.4												
QM F56233	COA	15.2	12.8												
QM F56234	COA	14.3	12.4												
QM F56138	KCB	15.1	15.1	16.3	14.2	14.1									
Neohelos stirtoni															
QM F40168*	Gag	17.5	16.1												
QM F40165*	Gag	17.1	14.4	17.8	15.6	16.3	20.2	18.0	18.2	22.2	21.2	18.6			
QM F40167*	HH	19.2													
Neohelos davidridei															
QM F40175*	JJ	20.7	16.6	20.5	17.1	18.0	23.0	20.2	19.1						
QM F40176*	JJ												21.0	20.4	15.5
QM F40178*	JJ	20.8	16.8												
QM F40181*	JJ				20.0										
QM F40186*	JJ									24.4	21.4				

Table B. *Neohelos* spp. lower dental measurements (in mm). Abbreviations: AW, anterior width; L, length; PW, posterior width; W, width. Specimens asterisked are taken from Murray et al. (2000).

Specimen	Site	p3		m1			m2			m3			m4		
		L	W	L	AW	PW	L	AW	PW	L	AW	PW	L	AW	PW
Neohelos tirarensis															
QM F41043*	D	12.0	8.4	15.3	10.5	11.6	16.0	12.3	12.7	17.0	13.0	12.2	16.2	12.1	10.5
QM F41044*	D	11.7	8.1	15.3	9.5	11.5	16.2	12.0	12.5	17.0	13.4	12.6	17.3	12.7	11.9
QM F40173*	SB	12.5	8.6	17.3	11.6	12.2									
QM F40028	BO			15.7	10.3	11.2									
QM F36535	BC2			17.5	10.7	12.2									
QM F56240	Wang						17.0	11.9	12.0						
QM F30868	NP			16.6	11.2	12.4									
QM F40155*	WW	13.0	10.0	17.4	10.8	12.2	18.5	13.9	14.4	18.7	15.4	14.4	18.2	14.1	13.9
QM F40157*	WW	11.5	8.1	16.5	10.5	11.8									
QM F40135*	CS	13.0	8.5												
QM F56235	CS	11.6	8.2												
QM F40139*	CS			17.8	12.0	13.7									
QM F40141*	CS			17.0	10.8	11.3									
QM F40148*	MM									19.2	14.2	13.6			
QM F40152*	NG									19.6	14.1	12.9			
QM F40154*	NG									19.7	14.9	13.8			
QM F12499*	NG			16.5	10.8	11.9									
QM F40146*	JJS									19.6	14.1	14.2			
QM F30383	KCB									19.9	13.5				
QM F30479	KCB	12.3	8.2												
QM F41200	KCB	13.4	8.5	16.4	12.6	13.3	18.7	15.5	14.5						
QM F56241	WH	12.5	8.5												
Neohelos solus															
QM F 40159*	COA			17.1	10.2	11.4									
QM F 40164*	COA			17.1	10.3	11.6									
QM F57284	COA			13.8	8.1	8.5	14.7	9.9							

Specimen	Site	p3		m1			m2			m3			m4		
		L	W	L	AW	PW	L	AW	PW	L	AW	PW	L	AW	PW
QM F56136	COA	11.7	8.0												
QM F20830*	COA						17.1	12.1	12.0						
QM F12432*	COA									18.5	12.6	12.2			
QM F20486*	COA			14.8	8.8	10.3									
QM F20489*	COA									16.8	13.0	12.8			
QM F20490*	COA									18.8	13.9	12.7			
QM F20491*	COA			14.7	9.7	10.3									
QM F20709*	COA									17.8	13.3	12.2			
QM F20832*	COA									18.0	12.0	11.2			
QM F20838*	COA			16.0	10.4	12.0									
QM F22766*	COA						17.6	12.7	12.5						
QM F22774*	COA	13.5	9.4												
QM F23198*	COA	14.1	9.1												
QM F23199*	COA	12.9	8.3												
QM F24230*	COA									17.2	12.5	12.0			
QM F24298*	COA	10.5	7.0												
QM F24300*	COA	12.0	8.5												
QM F24432*	COA			15.7	9.2	10.8									
QM F24433*	COA									17.2	12.2	12.0			
QM F24435*	COA			16.0	9.5	10.7									
QM F24440*	COA											11.8	17.4	13.3	10.7
QM F24667*	COA	11.0	7.4												
QM F29738*	COA	12.0	9.5												
QM F30231*	COA			16.8	10.2	11.3	17.3	12.6	12.5		14.4				
QM F30306*	COA						17.0	11.8	11.5						
QM F30554*	COA			17.0	10.0	11.7									
QM F30560*	COA			15.4	9.8	10.5									
QM F30819	COA									18.1	13.7	12.8	18.5	13.1	12.0
QM F30880	COA									17.6	13.4	12.7			
QM F31364	COA	12.8	8.0												
QM F31359	COA	12.1	8.2												
QM F36232	COA	12.1	8.7												
QM F31357	COA			16.4	10.1	11.1									
QM F31343	COA			16.2											
QM F31366	COA			15.3	10.0	10.3									
QM F50487	COA			15.8	10.7	11.7									
QM F50498	COA									20.6	14.9	13.6			
Neohelos davidridei															
QM F40182*	JJ	16.8	10.7												
QM F40174*	JJ			21.2		15.1	23.1	17.5		25.0					
QM F40180*	JJ			21.0											
QM F40176*	JJ						25.2	18.7	18.0	24.2	19.4	17.6			
QM F40178	JJ						22.2	16.7	16.5						
Neohelos stirtoni															
QM F40169*	HH	14.5	10.5												
QM F40170*	HH									22.2	16.7	16.4			
QM F40117	GS									22.6	17.7	17.5		19.5	

http://dx.doi.org/10.4202/app.2012.0001

Appendix 3

Description of additional material of *Neohelos solus*.

P3

QMF50481.—Unworn P3 that is narrower than the holotype yet still relatively broad. The protocone is well developed, the parastyle is small and erect and the hypocone is the smallest cusp, as in QMF30878. The mesostyle is similarly a faint, ridged swelling at the posterobuccal corner of the P3. The posterobuccal cingulum is also poorly developed.

QMF50488.—A larger and more robust P3 compared with the holotype. A moderate degree of wear is evident on the apices of the parametacone, parastyle, and protocone, as well as the anterolingual basin between the parastyle and parametacone. QMF50488 is similar to QMF30878 in its development of the major cusps although the posterolingual border of the tooth (including the hypocone) is missing. The mesostyle is slightly better differentiated and the posterobuccal cingulum is more distinct and contacts the posterior base of the mesostyle.

QM F56233.—A relatively unworn right P3 that is similar in size and morphology to QMF30878, except for the following: the hypocone is larger and connected to the base of the protocone by a short anteroposterior crest; the valley between the parastyle and the anterobuccal base of the parametacone is deeper; and the parastyle has a short anterobuccally directed crest from its apex.

QM F56232, QM F56234.—Right and left premolars, respectively, possibly from the same individual due to the almost identical morphology, degree of wear and state of preservation. Both premolars are lightly worn on the parametacone apex. They differ from QMF30878 in the following features: the hypocone is a slight swelling on the posterolingual cingulum; the parastyle is smaller but more erect and separated from the parametacone base; and the posterobuccal cingulum is better defined, whereas the mesostyle is similarly developed.

QM F56138.—The P3 of QM F56138 is slightly larger than the holotype, but with the same basic proportions, resulting in a subovate occlusal outline. It differs from the P3 of QMF30878 in: having a weaker posterobuccal parametacone crest; in lacking a hypocone; and in having a more distinct (yet still relatively weak) posterobuccal cingulum.

M1

QMF31356. Unworn M1 similar to QMF30878, except for the following features: the parastyle is larger and is connected to the paracone apex by the preparacrista; the postprotocrista is less strongly developed; the protoloph and metaloph exhibit a more parallel arrangement, however the protoloph is slightly more crescentic than the metaloph and possesses the posterior cleft specific to *Ne. solus* M1s.

QMF50486.—Unworn M1 similar to QMF30878, except for the following features: the anterobuccal tooth corner is more squared owing to a more cuspate parastyle; the anterior and posterior cingula are better developed; the postmetacrista is weaker; and the metastyle is more distinctly cuspate (such as in the referred QMF20852).

QM F56138.—Left M1 that differs from the holotype M1 in: being broader anteriorly; and in having a better developed parastyle and stylar cusp E. From the Cleft Of Ages sample, the M1 of QM F56138 is most similar to QMF24731 in overall shape and the relative development of cusps, crests and cingula.

M2

QMF50490, QMF50492.—Both are left M2s that are similar to QMF30878, except for the following features: the protoloph is wider than the metaloph (although this area is fractured in the holotype and may appear wider than it actually is); and the metastyle is reduced. In QMF50492, the parastyle is further reduced than in either QMF50490 or QMF30878.

M3

QMF50493.—A slightly worn left M3 that is relatively indistinguishable from the M3 of the holotype, except that the protoloph and metaloph are slightly more crescentic.

M4

QMF50494.—The M4 is similar to M3, except for a marked reduction in the metaloph.